

Compressible cell gas models for asymmetric fluid criticality

 Claudio A. Cerdeiriña^{1,*} and Gerassimos Orkoulas^{2,†}
¹*Departamento de Física Aplicada, Universidad de Vigo, Campus del Agua, Ourense 32004, Spain*
²*School of Engineering, Widener University, Chester, Pennsylvania 19013, USA*

(Received 12 December 2016; published 3 March 2017)

We thoroughly describe a class of models recently presented by Fisher and coworkers [Phys. Rev. Lett. **116**, 040601 (2016)]. The crucial feature of such models, termed *compressible cell gases* (CCGs), is that the individual cell volumes of a lattice gas are allowed to fluctuate. They are studied via the seldom-used (μ, p, T) ensemble, which leads to their exact mapping onto the Ising model. Remarkably, CCGs obey *complete scaling*, a formulation for the thermodynamic behavior of fluids near the gas-liquid critical point that accommodates features inherent to the asymmetric nature of this phase transition like the Yang-Yang (YY) and singular coexistence-curve diameter anomalies. The CCG₀ models generated when volumes vary freely reveal *local free volume fluctuations* as the origin of these phenomena. Local *energy-volume coupling* is found to be another relevant microscopic factor. Furthermore, the CCG class is greatly extended by using the decoration transformation, with an interesting example being the Sastry-Debenedetti-Sciortino-Stanley model for hydrogen bonding in low-temperature water. The magnitude of anomalies is characterized by a single parameter, the YY ratio, which for the models so far considered here ranges from $-\infty$ to $\frac{1}{2}$.

DOI: 10.1103/PhysRevE.95.032105

I. INTRODUCTION

Basic features of critical phenomena [1] are most frequently illustrated for the ferromagnetic-paramagnetic phase transition. Then, by exploiting well-known analogies, results are straightforwardly translated to gas-liquid criticality in pure fluids. Among other manifestations, this means that critical exponents characterizing power-law singularities of physical properties are the same for, e.g., the Curie point of nickel or the gas-liquid critical point of argon. They are indeed those for the three-dimensional Ising model of ferromagnetism, this being the reason why these two phase transitions are said to belong to the three-dimensional-Ising universality class.

There are, however, nontrivial differences between them. Notably, experiment has established that the obvious symmetry of the spontaneous magnetization curve upon magnetic field reversal is absent in its fluid analog, the gas-liquid coexistence curve. That was already expressed in the nineteenth century by what has been termed the Law of the Rectilinear Diameter, namely, that the midpoints of the phase boundary in the density-temperature $(\rho-T)$ plane fit to a straight line with, in general, a nonvanishing slope \bar{A}_1 :

$$\rho_d \equiv \frac{1}{2}(\rho^{\text{gas}} + \rho^{\text{liq}}) \sim \rho_c + \bar{A}_1(T - T_c), \quad (1.1)$$

where superscripts refer to gas and liquid coexisting phases and the subscript “c” denotes criticality. This is regarded as a “classical” law in that such behavior is predicted by van der Waals mean-field theory.

A major breakthrough in the topic of asymmetry in gas-liquid phase transitions originates in work fifty years ago by Yang and Yang [2], who focused their attention on an exact relation for the isochoric heat capacity, C_V , which in the two-

phase region can be expressed as

$$\frac{\rho}{\rho_c} C_V = \tilde{C}_p + \frac{\rho}{\rho_c} \tilde{C}_\mu, \quad (1.2)$$

where $v = 1/\rho = V/N$ is the volume per particle while $\tilde{C}_p \equiv v_c T d^2 p_\sigma / dT^2$ and $\tilde{C}_\mu \equiv -T d^2 \mu_\sigma / dT^2$, with p_σ and μ_σ the pressure and chemical potential at coexistence. At the critical isochore, $\rho = \rho_c$, one has asymptotically close to T_c

$$C_V \sim A^- |t|^{-\alpha}, \quad (1.3)$$

with $t \equiv (T - T_c)/T_c$, A^- a nonuniversal, system-dependent amplitude, and $\alpha \simeq 0.109$. Then, Yang and Yang stated that for real fluids it is more reasonable to expect that both \tilde{C}_p and \tilde{C}_μ contribute to the C_V divergence:

$$\tilde{C}_p \sim \tilde{A}_p^- |t|^{-\alpha} \quad \text{and} \quad \tilde{C}_\mu \sim \tilde{A}_\mu^- |t|^{-\alpha}. \quad (1.4)$$

In the early formulations of the thermodynamic behavior near the gas-liquid critical point [3,4] only \tilde{C}_p diverges, with the chemical potential remaining nonsingular (or analytic), that is, $\tilde{A}_\mu^- = 0$ so that $A^- = \tilde{A}_p^-$. Hence, the question was whether or not \tilde{C}_μ diverges. A definite answer came from experiment since, according to (1.2), in the two-phase region ρC_V is a linear function of ρ along an isotherm, with \tilde{C}_μ and $\rho_c \tilde{C}_p$ being, respectively, the slope and the intercept (see also Fig. 1). Explicitly, careful analysis of two-phase $C_V(\rho, T)$ data for CO₂ and propane in 2000 provided [5,6] evidence that both \tilde{C}_p and \tilde{C}_μ diverge, implying the existence of the so-called Yang-Yang (YY) anomaly. This led to *complete scaling* [5,7], the thermodynamic formulation that accommodates the YY anomaly, but also recently [8] to statistical mechanical models that illuminate the microscopic basis of this phenomenology.

More specifically, to quantify the magnitude of this effect, a Yang-Yang ratio \mathfrak{R}_μ was defined as

$$\mathfrak{R}_\mu \equiv \lim_{T \rightarrow T_c^-} \frac{\tilde{C}_\mu(T)}{\tilde{C}_p(T) + \tilde{C}_\mu(T)} = \frac{\tilde{A}_\mu^-}{\tilde{A}_p^- + \tilde{A}_\mu^-}. \quad (1.5)$$

*calvarez@uvigo.es

†gorkoulas@mail.widener.edu

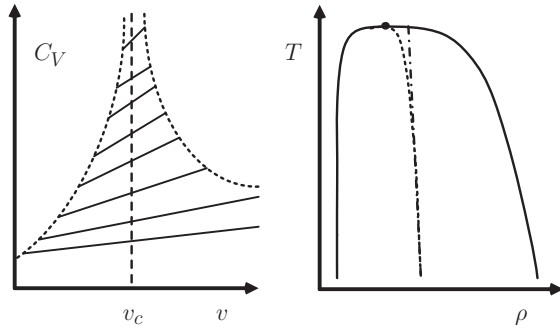


FIG. 1. Left: Two-phase isochoric heat capacity C_V as a function of volume $v = 1/\rho$ along isotherms (straight lines); the vertical dashed line corresponds to the critical isochore, along which C_V diverges, and the remaining dashed lines represent the phase boundaries (gas and liquid). Right: Coexistence curve in the temperature-density plane: the (real) diameter of the curve (dash) bends as the critical point is approached and so departs from a hypothetical rectilinear diameter (dot-dash). Both plots are obviously schematic.

One may realize (see Fig. 1 and Ref. [9]) that $\mathfrak{R}_\mu \neq 0$ whenever $A^{\text{liq}} \neq A^{\text{gas}}$, with these amplitudes characterizing the critical behavior of the heat capacity of gas and liquid coexisting phases: $C_V^{\text{gas}} \sim A^{\text{gas}}|t|^{-\alpha}$ and $C_V^{\text{liq}} \sim A^{\text{liq}}|t|^{-\alpha}$. Thus, the Yang-Yang anomaly has to do with the *asymmetry between gas and liquid*.

In this context, it is natural to expect that such an asymmetry manifests also in the density. In this connection, it was noted long ago that the diameter of the coexistence curve exhibits a $|t|^{1-\alpha}$ singularity [4] and thereby departs from linearity close to criticality (see Fig. 1 for illustration). But this is only a part of the overall situation. Indeed, complete scaling predicts the existence of a $|t|^{2\beta}$ term (with $\beta \simeq 0.326$) which asymptotically close to criticality dominates the previously anticipated $|t|^{1-\alpha}$ one since $2\beta < 1 - \alpha$ [10]. More generally, complete scaling contemplates a comprehensive set of critical anomalies associated with asymmetry [7]. Certainly, it is the scaling formulation of *asymmetric fluid criticality*.

While complete scaling was conceived from the analysis of two-phase C_V data of CO_2 and propane [5,6], it has received further support from similar studies for other fluids (see Ref. [9] for a recent account). Moreover, it has been shown that experiments [11–13] and simulations [11,14–16] on the asymptotic behavior of the coexistence-curve diameter demand a $|t|^{2\beta}$ singularity. The values estimated for \mathfrak{R}_μ from all these studies fall within the ranges imposed by the second law of thermodynamics [8]:

$$-\infty < \mathfrak{R}_\mu < 1. \quad (1.6)$$

In light of this background it is natural to ask what are the microscopic roots of YY features. One expects explicit responses to this question from statistical mechanical models. Nevertheless, in the *standard lattice gas* (SLG), on which much of our understanding of fluid criticality is based [17,18], $\mathfrak{R}_\mu \equiv 0$, this being also the situation for early models of asymmetric critical behavior of fluids [19,20].

Indeed, progress on this topic has been published only recently [8]. In doing so, Fisher and the present authors have introduced a new class of lattice-gas-like models, termed

compressible cell gases (CCGs), that exhibit Yang-Yang anomalies, $|t|^{2\beta}$ singularities in the coexistence-curve diameter, and related phenomena. A lattice gas can be interpreted as a *continuum model* in which space is divided in a regular arrangement of “cells” that can be empty or occupied, most commonly, by just one particle. The volume of such cells is constant for the SLG and usual variants. Conversely, the individual cell volumes are allowed to fluctuate in CCGs, this being their crucial feature. Working in the great grand canonical (GGC) or (μ, p, T) ensemble [21,22], such models are mapped onto the Ising model, and thereby they are regarded exactly soluble.

Attention in Ref. [8] was focused on CCG_0 models characterized by cell volumes that fluctuate freely. These constitute an important subclass and identify *local free volume fluctuations*, inherent to the disordered nature of real fluids while absent in lattice gases with cells of constant volume, as a microscopic source of YY and related anomalies. More elaborated versions generated using the *decoration transformation* [23,24] were explored. An interesting example is the Sastry-DeBenedetti-Sciortino-Stanley (SDSS or S^3D) compressible cell gas for hydrogen bonding in low-temperature water [25]. Such a model revealed the *coupling of local volumes and interaction energies* as relevant to \mathfrak{R}_μ .

Following up on Ref. [8], we analyze here the implications of CCGs for asymmetric fluid criticality. Before entering into detail, we summarize in Sec. II the specific predictions of complete scaling for \tilde{C}_p , \tilde{C}_μ , and ρ_d as well as the special properties of the GGC ensemble. A general analysis of CCG_0 models is presented in Sec. III. We first formulate them and show their exact mapping into the Ising model. Then we focus on the origin, sign, and magnitude of \mathfrak{R}_μ . A number of features of geometrical nature associated with local free volume fluctuations are highlighted. In addition, an enhanced CCG_0^+ model that incorporates energy-volume coupling is presented and the most basic aspects of calculations outlined. Decorated models are analyzed in Sec. IV. Besides a description of the decoration transformation in the GGC ensemble, a “simplest” decorated CCG and the S^3D are studied. We summarize in Sec. V all findings in a historical context. Appendices complete the details of the calculations.

II. ESSENTIAL BACKGROUND

A. Complete scaling

The distinction between “fields” and “densities” is essential for describing the thermodynamics of a system at near-criticality [26]. The field variables of a fluid are p , T , and μ but, because of asymmetry, one must employ redefined variables, termed *scaling fields*, that are algebraic combinations of them. There are three “relevant” scaling fields, \tilde{p} , \tilde{t} , and \tilde{h} , and a set of “irrelevant” scaling fields, from which one can define corresponding scaling variables, $y = U\tilde{h}/|\tilde{t}|^{2-\alpha-\beta}$, $y_k = U_k|\tilde{t}|^{\theta_k}$, with $U > 0$ and U_k nonuniversal, system-dependent amplitudes. These variables are the arguments of the scaling function W_\pm , where subscripts + and – apply to $\tilde{t} > 0$ and $\tilde{t} < 0$. The thermodynamics is then expressed as

$$\tilde{p} = Q|\tilde{t}|^{2-\alpha} W_\pm(y, y_4, y_5, \dots), \quad (2.1)$$

with $Q > 0$ another nonuniversal amplitude. The “relevant” scaling variable y serves to describe the leading singularities in the thermodynamic properties as well as those contributions arising from the asymmetric nature of the gas-liquid phase transition. On the other hand, y_4, y_5 , etc., account for the leading correction-to-scaling terms. Here only $y_4 = U_4 \tilde{t}^\theta$, with $\theta \simeq 0.52$, will be considered since odd arguments like y_5 are not present for the Ising-like models we will be dealing with. In doing so, we will approximate the amplitude U_4 by its critical value, U_{4c} .

The relevant scaling variable is small for the two paths of approach to the critical point to be explored, namely, critical isochore and coexistence. Thus, for $\tilde{t} > 0$ the following small- y expansion applies:

$$W_+ = W_{+0}^0 + W_{+2}^0 y^2 + \dots + U_{4c} W_{+0}^{(4)} |\tilde{t}^\theta + \dots, \quad (2.2)$$

while for $\tilde{t} < 0$ we have

$$W_- = W_{-0}^0 + W_{-1}^0 |y| + W_{-2}^0 y^2 + \dots + U_{4c} W_{-0}^{(4)} |\tilde{t}^\theta + \dots. \quad (2.3)$$

As explained in Ref. [27], we can take $W_{+0}^0 = W_{+2}^0 = 1$, $W_{-0}^0 \simeq 1.9$, $W_{-1}^0 \simeq 2.4$, $W_{-2}^0 \simeq 0.20$.

The *crucial feature of complete scaling* is that it expresses the scaling fields \tilde{p} , \tilde{t} , and \tilde{h} as combinations of *all* physical fields p , T , and μ . On defining $\check{p} \equiv (p - p_c)/\rho_c k_B T_c$ and $\check{\mu} \equiv (\mu - \mu_c)/k_B T_c$, one has to second order [7]

$$\tilde{p} = \check{p} - k_0 t - l_0 \check{\mu} - r_0 t^2 - q_0 \check{\mu}^2 - v_0 t \check{\mu} - m_0 \check{p}^2 - n_0 \check{p} \check{\mu} - n_3 \check{p} \check{\mu} + \dots, \quad (2.4)$$

$$\tilde{t} = t - l_1 \check{\mu} - j_1 \check{p} - r_1 t^2 - q_1 \check{\mu}^2 - v_1 t \check{\mu} - m_1 \check{p}^2 - n_1 \check{p} \check{\mu} - n_4 \check{p} \check{\mu} + \dots, \quad (2.5)$$

$$\tilde{h} = \check{\mu} - k_1 t - j_2 \check{p} - r_2 t^2 - q_2 \check{\mu}^2 - v_2 t \check{\mu} - m_2 \check{p}^2 - n_2 \check{p} \check{\mu} - n_5 \check{p} \check{\mu} + \dots, \quad (2.6)$$

where k_i, l_i , etc. are nonuniversal “mixing coefficients.”

As reported originally [7], $l_0 = 1$ and $k_0 = \mathcal{S}_c/\rho_c k_B$, with \mathcal{S} the entropy per unit volume. To describe the significance of the remaining mixing coefficients in (2.4) to (2.6)—especially those of the linear terms—let us focus on the predictions of complete scaling for the coexisting densities as well as the phase boundaries in the p - T and μ - T planes:

$$\rho^{\text{gas,liq}} = \rho_c [1 + A_{2\beta} |t|^{2\beta} + A_{1-\alpha} |t|^{1-\alpha} + A_1 |t| + \dots \pm B |t|^\beta (1 + b_\theta |t|^\theta + b_{2\beta} |t|^{2\beta} + \dots)], \quad (2.7)$$

$$\check{p}_\sigma(T) = \check{p}_{\sigma,1} t + \check{p}_{\sigma,2} t^2 + \check{A}_p^- |t|^{2-\alpha} [1 + \check{a}_p^- |t|^\theta + \dots], \quad (2.8)$$

$$\check{\mu}_\sigma(T) = \check{\mu}_{\sigma,1} t + \check{\mu}_{\sigma,2} t^2 + \check{A}_\mu^- |t|^{2-\alpha} [1 + \check{a}_\mu^- |t|^\theta + \dots], \quad (2.9)$$

where $A_1, \check{p}_{\sigma,1}, \check{p}_{\sigma,2}, \check{\mu}_{\sigma,1}$, and $\check{\mu}_{\sigma,2}$ depend exclusively on the mixing coefficients, b_θ, \check{a}_p^- , and \check{a}_μ^- are amplitudes that characterize correction-to-scaling terms, and $+$ and $-$ in the

second row of (2.7) refer to liquid and gas, respectively, while

$$B = (1 - j_2) Q U W_{-1}^0 |\tau|^\beta, \quad (2.10)$$

$$A_{2\beta} = -j_2 B^2 / (1 - j_2), \quad b_{2\beta} = j_2^2 B^2 / (1 - j_2)^2, \quad (2.11)$$

$$A_{1-\alpha} = (2 - \alpha)(l_1 + j_1) Q W_{-0}^0 |\tau|^{1-\alpha}, \quad (2.12)$$

$$A_1 = v_0 + n_3 + (2q_0 + n_0) \check{\mu}_{\sigma,1} + (n_0 + 2m_0) \check{p}_{\sigma,1}, \quad (2.13)$$

$$\check{A}_p^- = \frac{Q W_{-0}^0}{1 - j_2} |\tau|^{2-\alpha}, \quad \check{A}_\mu^- = j_2 \check{A}_p^-, \quad (2.14)$$

with

$$\tau = 1 - k_1 l_1 - \check{p}_{\sigma,1} (j_1 + j_2 l_1). \quad (2.15)$$

Equation (2.14) leads to the critical amplitudes of \check{C}_p and \check{C}_μ in (1.4):

$$\check{A}_p^- = (2 - \alpha)(1 - \alpha) k_B \check{A}_p^-, \quad \check{A}_\mu^- = -j_2 \check{A}_p^-. \quad (2.16)$$

As already discussed in the original formulation of scaling [3], $k_1 \neq 0$ in (2.6) suffices to account for $(d\mu_\sigma/dT)_c \neq 0$. On the other hand, the $|t|^{2\beta}$ and $|t|^{1-\alpha}$ singularities in (2.7) contribute to the diameter in (1.1). While the discovery of the latter led to the incorporation of μ mixing into the “thermal field” \tilde{t} [4], pressure mixing into \tilde{t} also generates a $|t|^{1-\alpha}$ singularity, as (2.12) reflects. Remarkably, Eq. (2.11) indicates that pressure mixing into the “ordering field” \tilde{h} , i.e., $j_2 \neq 0$, implies $A_{2\beta} \neq 0$. Also, from the combination of (1.5), (2.10), (2.11), and (2.16) one encounters

$$\mathfrak{X}_\mu = -j_2 / (1 - j_2) \quad \text{and} \quad A_{2\beta} = \mathfrak{X}_\mu B^2. \quad (2.17)$$

Thus, it is clear that *pressure mixing into \tilde{h} is crucial* in that it generates a nonvanishing YY ratio and the $|t|^{2\beta}$ singularity in ρ_d .

From the above information one finds

$$-\infty < j_2 < 1 \quad \text{and} \quad \check{A}_p^- > 0. \quad (2.18)$$

This means, from (1.4), that \check{C}_p always diverges to $+\infty$. Then (2.16) implies that $\check{C}_\mu \rightarrow +\infty$ when $j_2 < 0$ (or $\mathfrak{X}_\mu > 0$) whereas $\check{C}_\mu \rightarrow -\infty$ when $j_2 > 0$ (or $\mathfrak{X}_\mu < 0$). These two contrasting situations, observed experimentally [5,6,9], are illustrated in Figs. 2 and 3, which show numerical results for models presented in Sec. III [28]. There is more to be said about the details of complete scaling; the reader can consult Ref. [7].

B. Great grand canonical ensemble

According to Guggenheim [21], who introduced it, this is the statistical ensemble for a system with given temperature, pressure, and chemical potential, this being the reason why it is also known as the (μ, p, T) ensemble. While it was discussed in detail long ago [22], it merits some attention summarizing its special properties.

We start by noting that, according to Gibbs-Duhem equation,

$$0 = N d\mu - V dp + S dT, \quad (2.19)$$

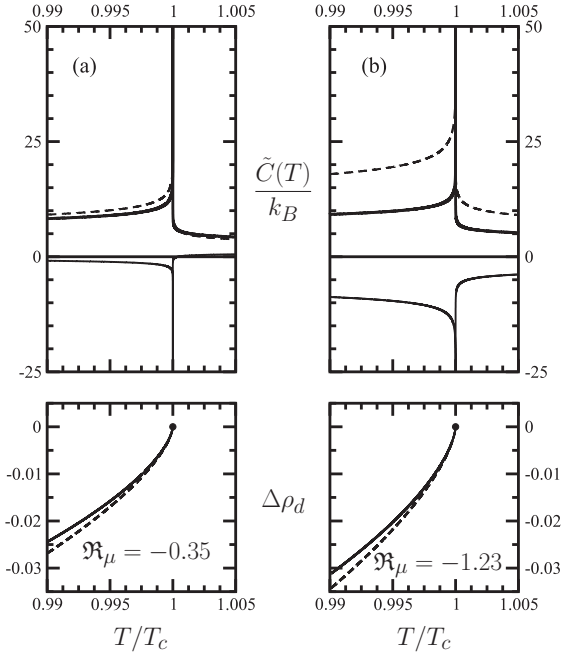


FIG. 2. Isochoric heat capacity $C_V(T)$ (bold solid) with its contributions $\tilde{C}_p(T)$ (dashed) and $\tilde{C}_\mu(T)$ (solid) and reduced coexistence-curve diameter $\Delta\rho_d(T) \equiv (\rho^{\text{liq}} + \rho^{\text{vap}})/2\rho_c - 1$ (solid) with its $|t|^{2\beta}$ singularity (dashed) along the critical isochore for simple-cubic-lattice CCG_0 models (described in Sec. III) with point particles ($w = 0$) and three available cell volumes: (a) $v_2 = 5v_1$, $v_3 = v_1$; (b) $v_2 = 50v_1$, $v_3 = v_1$. Results for $C_V(T)$, $\tilde{C}_p(T)$, and $\tilde{C}_\mu(T)$ contain background contributions as well as leading, asymmetry-related, and correction-to-scaling terms computed as described in Sec. III B.

it comes out that only two of μ , p , and T are independent in the thermodynamic limit, that is, $V \rightarrow \infty$, $N \rightarrow \infty$, and $S \rightarrow \infty$, with $\rho = N/V$ and $S = S/V$ finite.

This differential relation implies the existence of a function $L(\mu, p, T)$, which specifies the thermodynamics. Such function takes a constant value which one may arbitrarily choose to be 0, while, in addition, one has the freedom to consider that

$$\left(\frac{\partial L}{\partial \mu}\right)_{T,p} = \rho, \quad \left(\frac{\partial L}{\partial p}\right)_{T,\mu} = -1, \quad \left(\frac{\partial L}{\partial T}\right)_{p,\mu} = S. \quad (2.20)$$

Let us now focus on the grand canonical ensemble, in which the energy and number of particles are allowed to fluctuate. The partition function is

$$\Xi(\mu, V, T) = \sum_{N=0}^{\infty} e^{\beta\mu N} Z(N, V, T), \quad (2.21)$$

where $\beta \equiv 1/k_B T$ and Z is the canonical partition function, which embodies a sum over energy levels with Boltzmann factors $e^{-\beta E}$. In the thermodynamic limit

$$\frac{1}{\beta V} \ln \Xi = p(\mu, T), \quad \left(\frac{\partial p}{\partial \mu}\right)_T = \rho, \quad \left(\frac{\partial p}{\partial T}\right)_\mu = S. \quad (2.22)$$

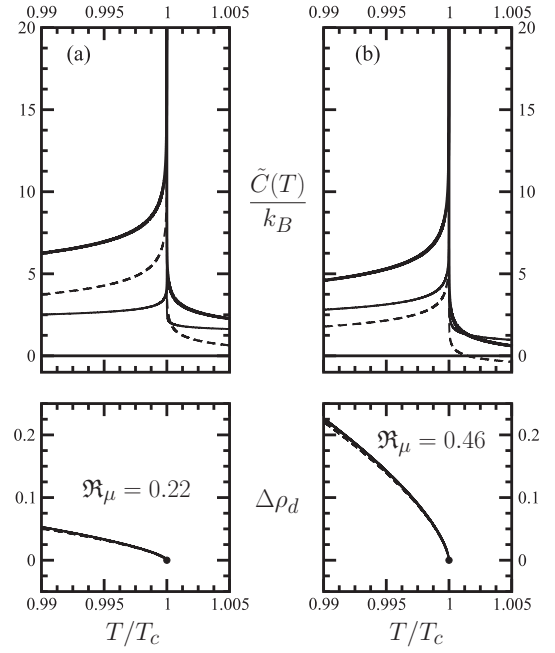


FIG. 3. Isochoric heat capacity $C_V(T)$ (bold solid) with its contributions $\tilde{C}_p(T)$ (dashed) and $\tilde{C}_\mu(T)$ (solid) and reduced coexistence-curve diameter $\Delta\rho_d(T) \equiv (\rho^{\text{liq}} + \rho^{\text{vap}})/2\rho_c - 1$ (solid) with its $|t|^{2\beta}$ singularity (dashed) along the critical isochore for simple-cubic-lattice CCG_0 models (described in Sec. III) with highly compressible particles and two available cell volumes: (a) $v_2 = v_1/5$, $v_3 = 5v_1$; (b) $v_2 = v_1/50$, $v_3 = 50v_1$. Results for $C_V(T)$, $\tilde{C}_p(T)$, and $\tilde{C}_\mu(T)$ contain background contributions as well as leading, asymmetry-related, and correction-to-scaling terms computed as described in Sec. III B.

To generate the *great* grand canonical (GGC) partition function Θ , we sum over volumes

$$\Theta = \int_0^\infty e^{-\bar{p}V} \Xi(\mu, V, \mu) \frac{dV}{V_0}, \quad (2.23)$$

where V_0 is a reference volume and $\bar{p} = p/k_B T$. As explained previously [22], the GGC partition function diverges so that, on defining

$$\Upsilon(\mu, p, T) \equiv -\frac{1}{\beta V_0 \Theta(\mu, p, T)} = p(\mu, T) - p = 0 \quad (2.24)$$

and using (2.22), one finds

$$\left(\frac{\partial \Upsilon}{\partial \mu}\right)_{T,p} = \rho, \quad \left(\frac{\partial \Upsilon}{\partial p}\right)_{T,\mu} = -1, \quad \left(\frac{\partial \Upsilon}{\partial T}\right)_{p,\mu} = S. \quad (2.25)$$

Comparison between (2.20) and (2.25) yields $\Upsilon = L$. Thus, knowledge of $\Theta(\mu, p, T)$ together with the condition that this function diverges leads to the thermodynamics of the system [29].

For the models considered in this work one may compute Θ from the partition function of a system of \mathcal{N} lattice sites (or

cells):

$$\Theta = \sum_{\mathcal{N}=0}^{\infty} \Theta_{\mathcal{N}}, \quad (2.26)$$

with

$$\Theta_{\mathcal{N}} = 1 \quad (2.27)$$

for values of \mathcal{N} that are sufficiently large (that is, macroscopic). This property of the GGC partition function, noted by Guggenheim [21], will be used in the next sections.

III. BASIC MODEL

A. Compressible cell gas

Consider the three-dimensional space divided into cells of constant volume v_0 whose centers are located at the \mathcal{N} sites of a lattice of coordination number c . To characterize repulsive or excluded volume effects, let us assume that each cell can be empty or accommodate a classical particle. Associated with any occupied cell is the “free volume” $\dot{v}_0 \leq v_0$ the center of its particle explores. Attractive interactions are considered, but, instead of being characterized by a normal pair potential, $\varphi(\mathbf{r}_i - \mathbf{r}_j)$, they are of fixed magnitude: the interaction energy is $-\varepsilon_0 < 0$ for particles in nearest-neighbor cells and 0 otherwise. Such a model is known as the nearest-neighbor standard lattice gas referred to in the Introduction. The grand canonical partition function is

$$\Xi^{\text{SLG}}(\mu, V, T) = \sum_{\{n_i\}} \exp \left[\bar{\beta} \varepsilon_0 \sum_{\langle ij \rangle} n_i n_j + \bar{\mu} \sum_{i=1}^{\mathcal{N}} n_i \right], \quad (3.1)$$

where $V = \mathcal{N}v_0$, $n_i = 0, 1$ is the occupancy number of cell i , $\langle ij \rangle$ indicates that the corresponding sum restricts to nearest-neighbor cells, and $\bar{\mu} = \beta\mu - \ln[\Lambda_T^3(T)/v_0]$. The definition of $\bar{\mu}$ absorbs, in the thermal de Broglie wavelength $\Lambda_T = \hbar\sqrt{2\pi/mk_B T}$ and the v_0 factor, the results of integrals over phase space for a system of classical particles of mass m . (Implicit is that point particles have been considered so that integrations over the volume accessible to the center of a particle in its cell yield a “local free volume” $\dot{v}_0 = v_0$ for each occupied cell.)

As a model for the gas-liquid phase transition, the SLG has played an important role in the development of the Modern Theory of Phase Transitions and Critical Phenomena. This is in large part because Ξ^{SLG} and Z^{Ising} , the canonical partition function of the Ising model, have the same mathematical structure [17]. Specifically

$$Z^{\text{Ising}}(H, \mathcal{N}, T) = \sum_{\{s_i\}} \exp \left[K \sum_{\langle ij \rangle} s_i s_j + h \sum_{i=1}^{\mathcal{N}} s_i \right], \quad (3.2)$$

where $s_i = -1, 1$ is the Ising variable characterizing the state (up or down) of spin i in the lattice, $K \equiv J/k_B T$, $h \equiv H/k_B T$ (with $J > 0$ and H the coupling constant and magnetic field, respectively), while the partition function is related to the free energy F via $\bar{f} \equiv -F/\mathcal{N}k_B T = \mathcal{N}^{-1} \ln Z^{\text{Ising}}$. Comparison between (3.1) and (3.2) yields the well-known SLG-Ising

model mapping:

$$\bar{f} = \bar{p}v_0 - \frac{c}{8}\bar{\beta}\varepsilon_0 - \frac{1}{2}\bar{\mu}, \quad K = \frac{1}{4}\bar{\beta}\varepsilon_0, \quad h = \frac{1}{2}\bar{\mu} + \frac{c}{4}\bar{\beta}\varepsilon_0. \quad (3.3)$$

Suppose now that the individual cell volumes of a SLG are allowed to take n discrete values, $0 < v_k \leq v_0$ ($k = 1, 2, \dots, n$) with corresponding free volumes $\dot{v}_k > 0$. One then has a compressible cell gas (CCG). The variants in which cell volumes fluctuate *independently* are termed CCG₀ models. One may anticipate that it is the condition that cell volumes fluctuate freely which allows the exact mapping of CCG₀s into the Ising model.

To describe such a mapping, it is useful to introduce the isobaric volume-fluctuation sums

$$S_{lm}(\bar{p}) = n^{-1} \sum_{k=1}^n v_k^l \dot{v}_k^m e^{-\bar{p}v_k}, \quad (3.4)$$

which contain the available volumes v_k and free volumes \dot{v}_k defined above [30]. Thus, each cell needs a $S_{00}(\bar{p})$ factor if vacant and a $e^{\bar{\mu}} S_{01}(\bar{p})$ factor if occupied. As a result,

$$\Theta_{\mathcal{N}}^{\text{CCG}_0} = S_{00}(\bar{p})^{\mathcal{N}} \sum_{\{n_i\}} \exp \left(\bar{\beta} \varepsilon_0 \sum_{\langle ij \rangle} n_i n_j + \left\{ \bar{\mu} + \ln \left[\frac{S_{01}(\bar{p})}{v_0 S_{00}(\bar{p})} \right] \right\}^{\sum_{i=1}^{\mathcal{N}} n_i} \right). \quad (3.5)$$

On using the first equation in (2.22) and (2.27), it becomes clear that the mathematical structure of Eqs. (3.1) and (3.5) is the same so that, with the aid of (3.3), the following CCG₀-Ising model mapping is found:

$$\bar{f} = -\frac{1}{2} \ln \left[\frac{S_{01}(\bar{p}) S_{00}(\bar{p})}{v_0} \right] - \frac{c}{8} \bar{\beta} \varepsilon_0 - \frac{1}{2} \bar{\mu}, \quad (3.6)$$

$$K = \frac{1}{4} \bar{\beta} \varepsilon_0, \quad h = \frac{1}{2} \bar{\mu} + \frac{c}{4} \bar{\beta} \varepsilon_0 + \frac{1}{2} \ln \left[\frac{S_{01}(\bar{p})}{v_0 S_{00}(\bar{p})} \right]. \quad (3.7)$$

To extract conclusions from (3.6) and (3.7) in connection to the “mixing scheme” embodied by (2.4) to (2.6), we anticipate some results of the next subsection (supplemented by the appendices). Thus, as a rule, the appearance of \bar{p} , $\bar{\beta}$, and $\bar{\mu}$ in the Ising scaling fields, \bar{f} , K , and h , is equivalent to that of p , T , and μ in \bar{p} , \bar{t} , and \bar{h} , the field variables in terms of which complete scaling is formulated. Specifically, that \bar{p} enters explicitly into h in (3.7) means that p enters into the “ordering field” \bar{h} in (2.6). This implies that $j_2 \neq 0$ and, by (2.17), that \mathfrak{R}_{μ} and $A_{2\beta}$ are also nonvanishing. Since \bar{p} appears in the S_{01}/S_{00} factor, it is concluded that *pressure mixing into \bar{h}* and the associated Yang-Yang and related anomalies emerge in lattice-gas-like models when the individual cell volumes are allowed to fluctuate [31,32].

On the other hand, the absence of \bar{p} and $\bar{\mu}$ in K implies that of p and μ in the “thermal field” \bar{t} and so $l_1 = j_1 = 0$. As a result, the CCG₀ shows no $|t|^{1-\alpha}$ singularity in the coexistence-curve diameter [recall (2.12)].

B. Outline of the calculations

Let us describe the procedure for obtaining information from a mapping like that of (3.6) and (3.7). On defining $\check{K} \equiv K/K_c$, $\Delta\bar{\beta} \equiv \bar{\beta} - \bar{\beta}_c$, etc., and $\bar{f}_\beta \equiv \partial\bar{f}/\partial\bar{\beta}$, etc., it comes out that (3.6) and (3.7) can be expanded to get

$$\begin{aligned} \bar{f} &= g_1(\bar{\beta}_c, \bar{\mu}_c, \bar{p}_c) + \bar{f}_\beta \Delta\bar{\beta} + \bar{f}_\mu \Delta\bar{\mu} + \bar{f}_p \Delta\bar{p} + \frac{1}{2} \bar{f}_{\beta\beta} \Delta\bar{\beta}^2 \\ &\quad + \frac{1}{2} \bar{f}_{\mu\mu} \Delta\bar{\mu}^2 + \frac{1}{2} \bar{f}_{pp} \Delta\bar{p}^2 + \bar{f}_{\beta\mu} \Delta\bar{\beta} \Delta\bar{\mu} + \bar{f}_{\beta p} \Delta\bar{\beta} \Delta\bar{p} + \bar{f}_{\mu p} \Delta\bar{\mu} \Delta\bar{p} + \dots, \end{aligned} \quad (3.8)$$

$$\begin{aligned} \check{K} &= g_2(\bar{\beta}_c, \bar{\mu}_c, \bar{p}_c) + \check{K}_\beta \Delta\bar{\beta} + \check{K}_\mu \Delta\bar{\mu} + \check{K}_p \Delta\bar{p} + \frac{1}{2} \check{K}_{\beta\beta} \Delta\bar{\beta}^2 + \frac{1}{2} \check{K}_{\mu\mu} \Delta\bar{\mu}^2 \\ &\quad + \frac{1}{2} \check{K}_{pp} \Delta\bar{p}^2 + \check{K}_{\beta\mu} \Delta\bar{\beta} \Delta\bar{\mu} + \check{K}_{\beta p} \Delta\bar{\beta} \Delta\bar{p} + \check{K}_{\mu p} \Delta\bar{\mu} \Delta\bar{p} + \dots, \end{aligned} \quad (3.9)$$

$$\begin{aligned} h &= g_3(\bar{\beta}_c, \bar{\mu}_c, \bar{p}_c) + h_\beta \Delta\bar{\beta} + h_\mu \Delta\bar{\mu} + h_p \Delta\bar{p} + \frac{1}{2} h_{\beta\beta} \Delta\bar{\beta}^2 \\ &\quad + \frac{1}{2} h_{\mu\mu} \Delta\bar{\mu}^2 + \frac{1}{2} h_{pp} \Delta\bar{p}^2 + h_{\beta\mu} \Delta\bar{\beta} \Delta\bar{\mu} + h_{\beta p} \Delta\bar{\beta} \Delta\bar{p} + h_{\mu p} \Delta\bar{\mu} \Delta\bar{p} + \dots, \end{aligned} \quad (3.10)$$

where \bar{f}_β , etc. are evaluated at criticality.

The results for the underlying Ising model form the background information in these equations. In particular, one needs the critical coordinates, \bar{f}_c and K_c , and the expressions for the heat capacity and the magnetization at $h = 0$. We have taken that information from Liu and Fisher [33], who reported reliable values for the simple cubic, face-centered cubic, and body-centered cubic regular assemblies. The expressions for the heat capacity, magnetization, and some related properties are listed in Appendix A. Furthermore, Appendices B and C show general expressions that relate critical amplitudes Q , U , etc. and mixing coefficients to the critical values of the derivatives in (3.8) and (3.10) and the critical coordinates and critical amplitudes of the Ising lattice. Obviously, $\bar{\mu}_c$, \bar{p}_c , and $\bar{\beta}_c$ are needed.

With this preamble, we are ready to illustrate how the information plotted in Figs. 2 and 3 is obtained. Hence we consider a CCG model characterized by a concrete set of parameters (distribution of cell volumes, etc.). By specifying the values of such parameters, one first solves the following equations for $\bar{\mu}_c$, \bar{p}_c , and $\bar{\beta}_c$:

$$g_1(\bar{\beta}_c, \bar{\mu}_c, \bar{p}_c) = \bar{f}_c, \quad g_2(\bar{\beta}_c, \bar{\mu}_c, \bar{p}_c) = 1, \quad g_3(\bar{\beta}_c, \bar{\mu}_c, \bar{p}_c) = 0, \quad (3.11)$$

where implicit is that $\check{K}_c = 1$ and $h_c = 0$. Second, algebraic expressions for the derivatives in (3.8) to (3.10) must be obtained. (Results for all models under consideration are displayed in Appendices D and E.) According to Appendices B and C, these derivatives lead to j_2 , Q , etc., which, in turn, allow the obtainment of numerical values for $C_V(T)$, $\check{C}_p(T)$, $\check{C}_\mu(T)$, and $\rho_d(T)$ defined in Secs. I and II A. Since such data have been calculated on approaching the critical point along the critical isochore, $\rho = \rho_c$, only Ising results at $h = 0$ are needed [28,34].

C. Local free volume fluctuations

Let us now focus on the origin, sign, and magnitude of the crucial mixing coefficient j_2 and the closely related YY ratio \mathfrak{R}_μ for CCG₀ models. To that purpose, Eqs. (B26), (B8), (B29), and (2.17) are used to obtain an algebraic expression. By introducing the following averages taken over microstates

accessible to an individual cell

$$\langle v^l \dot{v}^m \rangle = \frac{S_{lm}(\bar{p}_c)}{S_{00}(\bar{p}_c)}, \quad (3.12)$$

one gets

$$\mathfrak{R}_\mu = -\frac{1}{2} \frac{\langle v \dot{v} \rangle - \langle v \rangle \langle \dot{v} \rangle}{\langle v \rangle \langle \dot{v} \rangle}. \quad (3.13)$$

Inspection of this equation leads to $-\infty < \mathfrak{R}_\mu < \frac{1}{2}$ (or $-1 < j_2 < 1$) as, in principle, the allowed range for the YY ratio for CCG₀ models, with $\mathfrak{R}_\mu \rightarrow -\infty$ when $\langle v \dot{v} \rangle$ numerically dominates the numerator of (3.13) and $\mathfrak{R}_\mu \rightarrow \frac{1}{2}$ when $\langle v \rangle \langle \dot{v} \rangle$ does. On the other hand, for constant free volumes, that is, $\dot{v}_k = \dot{v}_0$ for all k , one gets $\mathfrak{R}_\mu \equiv 0$. Therefore, as an important result, one finds that a nonvanishing YY ratio in the CCC₀ is a consequence of *local free volume fluctuations*.

To see how the above ranges are covered, let us start with the case of point particles, for which $\langle \dot{v} \rangle = \langle v \rangle$. From (3.13) one finds

$$\mathfrak{R}_\mu = -\frac{1}{2} \frac{\langle (\Delta v)^2 \rangle}{\langle v \rangle^2}, \quad (3.14)$$

where $\Delta v \equiv v - \langle v \rangle$. Clearly, this yields only negative values for \mathfrak{R}_μ . For the simple cubic lattice and two cell volumes, v_1 and $v_2 = \vartheta v_1$ (with $\vartheta > 1$) one finds $-0.63 < \mathfrak{R}_\mu < 0$ (or $0 < j_2 < 0.38$). Broad enough cell-volume distributions yield $|\mathfrak{R}_\mu|$ unbounded since one has the freedom of choosing the second moment indefinitely large relative to the mean.

Figure 2 illustrates the overall picture. As indicated at the end of Sec. II A, $\mathfrak{R}_\mu < 0$ (or $j_2 > 0$) implies that $\check{C}_\mu \rightarrow -\infty$. Since $A_{1-\alpha} \propto (l_1 + j_1) = 0$ for this model and $A_{2\beta} < 0$ [see (2.11) the coexistence-curve diameter curves towards higher densities near T_c . This is contrary to many experimental observations and simulations which evidence that ρ_d curves towards lower densities as the critical point is approached [11–16].

A natural extension is to consider that, more realistically, particles have a fixed size so that $\dot{v}_k = v_k - w$, with $w > 0$. For such “hard-core” particles one obtains from (3.13)

$$\mathfrak{R}_\mu = -\frac{1}{2} \frac{\langle (\Delta v)^2 \rangle}{\langle v \rangle (\langle v \rangle - w)}. \quad (3.15)$$

Again, only negative \mathfrak{R}_μ values are found, while numerical work indicates that, for the same cell volume distribution, the YY ratio is increased with respect to the case of point particles.

Now suppose that cell volumes and free volumes are allowed to vary independently. To explore this situation it is very informative to work out the case of just two cell volumes, i.e., $n = 2$. From (3.13) one finds

$$\mathfrak{R}_\mu = -\frac{1}{2} \frac{(v_1 - v_2)(\dot{v}_1 - \dot{v}_2)\pi_1\pi_2}{v_1\dot{v}_1\pi_1^2 + v_2\dot{v}_2\pi_2^2 + (v_1\dot{v}_2 + \dot{v}_1v_2)\pi_1\pi_2}, \quad (3.16)$$

where

$$\pi_1 = \frac{e^{-\bar{p}_c v_1}}{e^{-\bar{p}_c v_1} + e^{-\bar{p}_c \dot{v}_1}}, \quad \pi_2 = \frac{e^{-\bar{p}_c v_2}}{e^{-\bar{p}_c v_2} + e^{-\bar{p}_c \dot{v}_2}} \quad (3.17)$$

are the statistical weights. The denominator in (3.16) is positive, hence it comes out that \mathfrak{R}_μ is negative when cell volumes and free volumes are *correlated* ($v_1 > v_2 \Leftrightarrow \dot{v}_1 > \dot{v}_2$) and positive when they are *anticorrelated* ($v_1 > v_2 \Leftrightarrow \dot{v}_1 < \dot{v}_2$).

The YY ratio is negative for point particles and hard-core particles since cell volumes and free volumes are correlated (while they do not vary independently). Anticorrelation can be featured by considering that particles are ‘‘highly compressible’’ in that their effective volume varies so rapidly that they explore a larger volume in smaller cells. For instance, if $v_2 = \vartheta v_1$ and $\dot{v}_2 = \vartheta^{-1} \dot{v}_1$ (with $\vartheta < 1$), we find from (3.16)

$$\mathfrak{R}_\mu = \frac{1}{2} \frac{(\vartheta + \vartheta^{-1} - 2)\pi_1\pi_2}{(\vartheta + \vartheta^{-1} - 2)\pi_1\pi_2 + 1}, \quad (3.18)$$

which gives $0 < \mathfrak{R}_\mu < \frac{1}{2}$ (or $-1 < j_2 < 0$), with $\mathfrak{R}_\mu = \frac{1}{2} + O(\vartheta)$ when $\vartheta \rightarrow 0$. Figure 3 shows how these features manifest in the Yang-Yang anomaly and the coexistence-curve diameter: as can be seen, now ρ_d bends towards lower densities as $T \rightarrow T_c$.

While not explicitly stated, we have so far assumed that cells are of fixed shape. Alternatively, one may think of hard-core particles in cells of varying shape. As an example, let us consider the case of cubic particles with edge a and two cell shapes: (1) cubic with edge bL ($L > 1$) and (2) parallelepiped with two edges of length b and a third one of length $b[\cos \psi]^{-1}$ (see Fig. 4). By noting that $v_1 = b^3 L^3$ and $v_2 = b^3$, Eq. (3.16) can be written as

$$\mathfrak{R}_\mu = -\frac{1}{2} \frac{(L^3 - 1)(\dot{v}_1 - \dot{v}_2)\pi_1\pi_2}{\dot{v}_2\pi_2^2 + \dot{v}_1\pi_1\pi_2 + L^3(\dot{v}_1\pi_1^2 + \dot{v}_2\pi_1\pi_2)}, \quad (3.19)$$

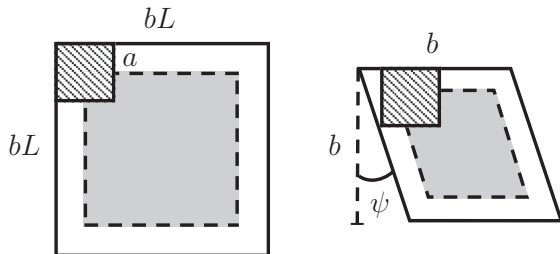


FIG. 4. Cross sections of cubic and parallelepiped cells with cubic particles of fixed volume and size in (see Sec. III C for a more detailed description). The shaded portions delimited by dashed lines are the ‘‘free volumes’’ particles explore.

where $\dot{v}_1 = (bL - 2a)^3$ and $\dot{v}_2 = (b - 2a)^2[b - 2a(1 + \tan \psi)]$. Since \dot{v}_2 decreases as ψ is increased up to a limiting value $\psi_{\max} = \arctan(b/2a - 1)$ for which $\dot{v}_2 = 0$, we have that $\dot{v}_1 > \dot{v}_2$. And numerical work indicates that, for the simple cubic lattice, $-0.63 < \mathfrak{R}_\mu < 0$ for any fixed value of $\psi < \psi_{\max}$. Since we are dealing with two cell volumes that are correlated with two free volumes, it is not surprising to find exactly the same numerical result quoted before.

While maintaining the geometry, let us now consider $v_1 = b^3$ and $v_2 = b^3 L^3$, with $L > 1$. This gives

$$\mathfrak{R}_\mu = \frac{1}{2} \frac{(L^3 - 1)(\dot{v}_1 - \dot{v}_2)\pi_1\pi_2}{\dot{v}_1\pi_1^2 + \dot{v}_2\pi_1\pi_2 + L^3(\dot{v}_2\pi_2^2 + \dot{v}_1\pi_1\pi_2)}, \quad (3.20)$$

where, now, $\dot{v}_1 = (b - 2a)^3$ and $\dot{v}_2 = (bL - 2a)^2[bL - 2a(1 + \tan \psi)]$. When $\psi = 0$, free volumes and cell volumes are correlated since $\dot{v}_1 < \dot{v}_2$. But \dot{v}_2 can be made arbitrarily small by increasing ψ up to its limiting value $\psi_{\max} = \arctan(bL/2a - 1)$, so there is an angle ψ_0 for which $\dot{v}_1 = \dot{v}_2$. Thus, free volumes are anticorrelated with cell volumes when $\psi_0 < \psi < \psi_{\max}$. For this range of ψ values, (3.20) yields $0 < \mathfrak{R}_\mu < \frac{1}{2}$, with $\mathfrak{R}_\mu \rightarrow \frac{1}{2}$ as $L \rightarrow \infty$.

Therefore, hard-core particles in cells of varying shape (and volume) can mimic either correlation or anticorrelation of cell volumes and free volumes. Although not discussed here, changes in particle shape could also be considered, thus giving rise to augmented models in which both volume and shape varies for cells but also for particles.

D. Energy-volume coupling

As an extension of the CCG₀, let us consider that a particle in a cell acquires a potential energy which depends on cell volume. The state of a cell in this CCG₀⁺ model is, as for the CCG₀, characterized by its volume v_k when empty and, additionally, by its free volume \dot{v}_k when occupied. But, furthermore, an energy ε_k is coupled to v_k and \dot{v}_k for occupied cells. Because of this extra energy, we need to introduce

$$S_{lmo}^+(\bar{p}, \bar{\beta}) = n^{-1} \sum_{k=1}^n v_k^l \dot{v}_k^m \varepsilon_k^o e^{-\bar{\beta} \varepsilon_k - \bar{p} v_k} \quad (3.21)$$

and

$$\langle v^l \dot{v}^m \varepsilon^o \rangle^+ = \frac{S_{lmo}^+(\bar{p}_c, \bar{\beta}_c)}{S_{000}^+(\bar{p}_c, \bar{\beta}_c)}, \quad (3.22)$$

so that (3.6) and (3.7) remain basically the same with S_{010}^+ substituting S_{01} and

$$\mathfrak{R}_\mu = -\frac{1}{2} \frac{\langle v \dot{v} \rangle^+ - \langle v \rangle^- \langle \dot{v} \rangle^+}{\langle v \rangle^- \langle \dot{v} \rangle^+}, \quad (3.23)$$

where mean values when an individual cell is occupied (+) or empty (−) are now distinct.

Nothing new regarding l_1 , j_1 , and the range of \mathfrak{R}_μ is found. It is interesting, however, to discuss the case of constant free

volumes. When $v_k = v_0$ for all k , Eq. (3.23) reduces to $\mathfrak{R}_\mu = \frac{1}{2}(\langle v \rangle^- - \langle v \rangle^+) / \langle v \rangle^-$. Thus, owing to the extra energies ε_k , \mathfrak{R}_μ is nonzero even for constant free volumes. One may note that the isobaric-isothermal volume-energy-fluctuation sums in (3.21) contain $e^{-\bar{\beta}\varepsilon_k - \bar{p}v_k}$ factors. It follows, then, that $\mathfrak{R}_\mu > 0$ emerges when lower v_k in (+) cells are statistically favored, that is, when the v_k and ε_k are correlated; conversely, $\mathfrak{R}_\mu < 0$ for anticorrelation. We conclude that, in addition to local free volume fluctuations, *the coupling between cell volume and particle energy is a source of nonvanishing YY ratios.*

IV. DECORATED VERSIONS

A. General formulation

It was noted long ago that the Ising model can be greatly extended by introducing extra spins at the midpoints of the $\frac{c}{2}\mathcal{N}$ bonds joining adjacent lattice sites [23,24]. Such models can be mapped into the basic, “undecorated” Ising model. The whole scheme is known as the decoration transformation. Transformed, decorated lattice gases have been studied in the past to study asymmetric fluid criticality [4,19,20,35,36].

A CCG₀ model with added cells may be called a decorated CCG₀ if extra cells contain up to one particle while their volume fluctuates freely (see Fig. 5 for a schematic illustration of a vertex-bond cell assembly). But instead of this most intuitive choice for the decorating system, it is more general and useful to consider an *arbitrary* system. This is the essence of the generalized decoration transformation [23].

Since the summations over the states of the decorating system can be performed individually and before the summations over the cells located at the vertex sites of the

lattice, a decorated CCG model can be reduced algebraically to an undecorated CCG₀ model with transformed variables $\bar{\mu}'$, \bar{p}' , and $\bar{\beta}'$. That entails the introduction of the so-called decorating factors, Ψ_{++} , Ψ_{--} , and Ψ_{+-} , which result from the summations for the decorating system over states in which “outer” cells are both occupied (++) , both empty (--) , and only one occupied (+-) [37]. Specifically, we may write for a vertex-bond cell assembly

$$e^{\bar{\beta}'\varepsilon_0} [e^{\bar{\mu}} S_{01}(\bar{p})]^{2/c} \Psi_{++} = e^{\bar{\beta}'\varepsilon_0} [e^{\bar{\mu}'} S_{01}(\bar{p}')]^{2/c}, \quad (4.1)$$

$$[e^{\bar{\mu}} S_{01}(\bar{p})]^{1/c} S_{00}(\bar{p})^{1/c} \Psi_{+-} = [e^{\bar{\mu}'} S_{01}(\bar{p}')]^{1/c} S_{00}(\bar{p}')^{1/c}, \quad (4.2)$$

$$S_{00}(\bar{p})^{2/c} \Psi_{--} = S_{00}(\bar{p}')^{2/c}, \quad (4.3)$$

where $2/c$ and $1/c$ have been introduced to avoid overcounting when extending the calculation to the whole system.

On combining (4.1) to (4.3) one gets

$$\bar{\beta}'\varepsilon_0 = \bar{\beta}\varepsilon_0 + \ln\left(\frac{\Psi_{++}\Psi_{--}}{\Psi_{+-}^2}\right), \quad (4.4)$$

$$\bar{\mu}' + \ln\left(\frac{S'_{01}}{v_0 S'_{00}}\right) = \bar{\mu} + \ln\left(\frac{S_{01}}{v_0 S_{00}}\right) + c \ln\left(\frac{\Psi_{+-}}{\Psi_{--}}\right), \quad (4.5)$$

$$\ln(S'_{00}) = \ln(S_{00}) + \frac{c}{2} \ln(\Psi_{--}), \quad (4.6)$$

so that with the aid of (3.6) and (3.7) we finally have

$$\begin{aligned} \bar{f} = & -\frac{1}{2} \ln\left[\frac{S_{01}(\bar{p})S_{00}(\bar{p})}{v_0}\right] - \frac{c}{8}\bar{\beta}\varepsilon_0 - \frac{1}{2}\bar{\mu} \\ & - \frac{c}{8} \ln(\Psi_{++}\Psi_{--}\Psi_{+-}^2), \end{aligned} \quad (4.7)$$

$$K = \frac{1}{4}\bar{\beta}\varepsilon_0 + \frac{1}{4} \ln\left(\frac{\Psi_{++}\Psi_{--}}{\Psi_{+-}^2}\right), \quad (4.8)$$

$$h = \frac{1}{2}\bar{\mu} + \frac{c}{4}\bar{\beta}\varepsilon_0 + \frac{1}{2} \ln\left[\frac{S_{01}(\bar{p})}{v_0 S_{00}(\bar{p})}\right] + \frac{c}{4} \ln\left(\frac{\Psi_{++}}{\Psi_{--}}\right). \quad (4.9)$$

Therefore, we have the CCG₀-Ising model mapping of (3.6) and (3.7) supplemented by extra terms arising from the decorating factors. Clearly, that Ψ_{++} depends on both \bar{p} and $\bar{\mu}$ is a sufficient condition for \bar{f} , K , and h to depend on all physical fields. Following the rules described at the end of Sec. III A, this implies that μ , p , and T enter into \tilde{h} , \tilde{p} , and \tilde{t} , so that complete scaling is obeyed in *all* its aspects.

B. Simplest model

It is natural to think first of CCG₀ models with decorating cells whose volume varies freely and contains up to one particle (see Fig. 5). In the simplest case, the sets of available volumes for decorating cells and the corresponding free volumes are the same as those for vertex cells. Accordingly, the decorating

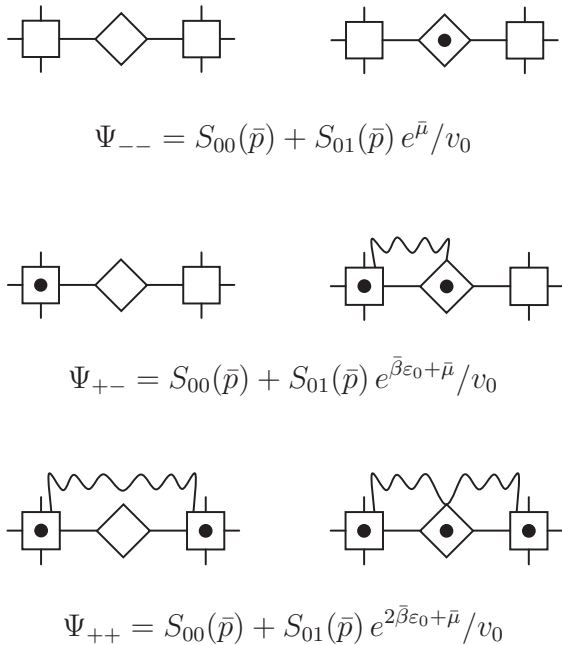


FIG. 5. Vertex-bond cell assembly in (---), (-+-), (+--), (++) , (+-+), and (+++) possible configurations for the “simplest” decorated CCG described in Sec. IV B. Decorating factors entering in (4.7) to (4.9) are also shown.

factors in (4.7) to (4.9) are

$$\Psi_{--} = S_{00}(\bar{p}) + \frac{1}{v_0} S_{01}(\bar{p}) e^{\bar{\mu}}, \quad (4.10)$$

$$\Psi_{+-} = S_{00}(\bar{p}) + \frac{1}{v_0} S_{01}(\bar{p}) e^{\beta \varepsilon_0 + \bar{\mu}}, \quad (4.11)$$

$$\Psi_{++} = S_{00}(\bar{p}) + \frac{1}{v_0} S_{01}(\bar{p}) e^{2\beta \varepsilon_0 + \bar{\mu}}. \quad (4.12)$$

From the inspection of (4.7) to (4.12) it comes clear that j_2 , j_1 , and l_1 are all nonvanishing. For fixed cell volumes this reduces to Mermin decorated lattice gas [20], which, among others, supported in the early 1970s $l_1 \neq 0$ and so a $|t|^{1-\alpha}$ singularity in the coexistence-curve diameter [4]. A nonvanishing pressure mixing coefficient j_1 that also contributes to the amplitude of the $|t|^{1-\alpha}$ singularity in (2.12) arises—as has been shown to be the case of j_2 —from local volume fluctuations; more specifically, $j_1 \neq 0$ when the volume of decorating cells is allowed to fluctuate.

By defining $\Psi_{++}^{\bar{p}} \equiv (\partial \Psi_{++} / \partial \bar{p})_{\bar{p}, \bar{\mu}}$ etc. and proceeding as explained at the beginning of Sec. III C (see also Appendix D) one finds

$$j_2 = \rho_c \frac{\frac{S_{11}}{S_{01}} - \frac{S_{10}}{S_{00}} - \frac{c}{2} \left(\frac{\Psi_{++}^{\bar{p}}}{\Psi_{++}} - \frac{\Psi_{--}^{\bar{p}}}{\Psi_{--}} \right)}{1 + \frac{c}{2} \left(\frac{\Psi_{++}^{\bar{\mu}}}{\Psi_{++}} - \frac{\Psi_{--}^{\bar{\mu}}}{\Psi_{--}} \right)}, \quad (4.13)$$

with, recall, all quantities evaluated at criticality. As expected, as for the (undecorated) CCG₀, one gets $-1 < j_2 < 1$ (or $-\infty < \mathfrak{R}_\mu < \frac{1}{2}$). Also consistently with the undecorated version of the model, one may verify from (4.13) that the YY ratio vanishes for the case of constant free volumes.

Following up on this simplest decorated CCG₀ model, more elaborated versions can be devised by supposing, e.g., that bond-cell volumes and bond-cell free volumes are distinct from those of outer cells, or that bond cells can accommodate an arbitrary number of particles that interact themselves and with particles in outer cells in a variety of ways, or that there exist alternative ways in which energy, number of particles, and volumes are coupled, etc. Evidently, decorated compressible cell gases constitute a *flexible* subclass of models.

C. Sastry-Debenedetti-Sciortino-Stanley model

This is a compressible cell gas, termed S³D model, originally devised [25] to account for the anomalous thermodynamics of liquid water at low temperatures [38]. As has been shown [8], it can be formulated as a decorated CCG.

One considers a lattice with vertex cells that, as in the SLG, are of fixed volume and can accommodate a particle that interacts with particles in nearest-neighbor cells via an energy $-\varepsilon_0$. To implement the orientational selectivity characteristic of hydrogen bonding, one supposes that there are q microstates for a particle, with only q of the q^2 joint configurations for particles in nearest-neighbor cells leading to the formation of a hydrogen bond which lowers the energy by $\delta\varepsilon > 0$. Furthermore, hydrogen bonding in low-temperature water, characterized by low-density, ice-like structures, requires an optimal interparticle separation. This is implemented by simply assuming that an assembly of two nearest-neighbor cells gains a volume $v_+ > 0$ in such states. As illustrated in

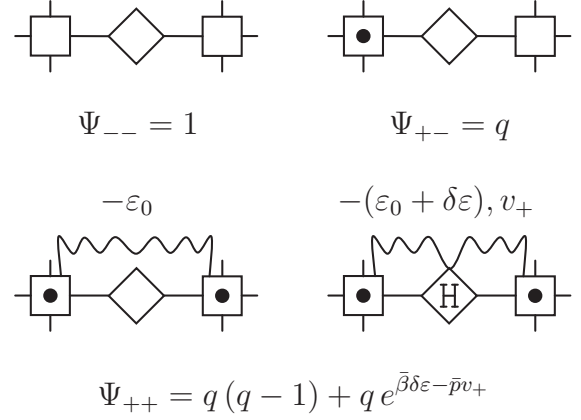


FIG. 6. Vertex-bond cell assembly for the S³D decorated model described in Sec. IV C. Decorating factors entering in (4.7) to (4.9) are also shown.

Fig. 6, these features can be implemented using a decorating system. Accordingly,

$$\Psi_{++} = q(q-1) + q e^{\beta \delta \varepsilon - \bar{p} v_+}, \quad (4.14)$$

$$\Psi_{+-} = q \quad \text{and} \quad \Psi_{--} = 1, \quad (4.15)$$

where implicit is that the free volume explored by individual particles remains the same for all states.

Introduction of these decorating factors in (4.7) to (4.9) leads to the conclusion that $l_1 = 0$ while appropriate calculations (see Appendix E) yield $j_1 \propto v_+$, that is, there is no μ mixing in the thermal scaling field \tilde{t} whereas the model contemplates pressure mixing and thereby a nonvanishing $|t|^{1-\alpha}$ singularity. Furthermore, for the crucial pressure mixing coefficient one finds

$$j_2 = \frac{1}{2} \rho_c v_+ e^{\beta \delta \varepsilon - \bar{p}_c v_+} / (q - 1 + e^{\beta \delta \varepsilon - \bar{p}_c v_+}). \quad (4.16)$$

Clearly $j_2 > 0$ or, according to (2.17), $\mathfrak{R}_\mu < 0$, and numerical work demonstrates that the model yields all negative values of the YY ratio.

It is important to remark that volumes are coupled with interaction energies in this model. Thus, as found in Sec. III D for the CCG₀⁺, *energy-volume coupling* results in nonvanishing YY and related anomalies. And also in accord with the CCG₀⁺, negative \mathfrak{R}_μ values are found when energies and volumes are anticorrelated.

A modified version in which interaction energies and volumes are correlated yields $\mathfrak{R}_\mu > 0$. This is achieved by simply considering in (4.16) that $v_+ < 0$, meaning that the formation of a hydrogen bond effectively reduces the volume available to a pair of neighboring particles. This leads to the obvious constraint $|v_+| < 2v_0/c$ and, since we are supposing that individual particles explore a constant volume v_0 , the reduced volume is shared. Numerical work for a simple cubic lattice with $q = 10$ reveals that $0 < \mathfrak{R}_\mu < 0.26$ but an upper bound $\mathfrak{R}_\mu = 0.43$ for $q = 1$.

V. SUMMARY IN A HISTORICAL CONTEXT

The 1962 experiments for argon [39] definitely led to the conclusion that the isochoric heat capacity C_V of pure substances diverges at the gas-liquid critical point. Only two years later, Yang and Yang [2] derived the thermodynamic relation (1.2) and posed the question whether both \tilde{C}_p and \tilde{C}_μ diverge. Being a straightforward translation of the Ising model [17], only \tilde{C}_p diverges in the standard lattice gas, which displays a fully symmetric coexistence curve in the density-temperature plane.

During the 1970s it was concluded that there was no conclusive experimental evidence for \tilde{C}_μ diverging at criticality. Simultaneously, statistical mechanical models [4,19,20] revealed the existence of a $|t|^{1-\alpha}$ term that results in a “hooked” coexistence-curve diameter close to the critical point. And it was soon claimed that experiments confirmed such a deviation from the Law of the Rectilinear Diameter [40]. The original scaling formulation [3] was then extended to accommodate the $|t|^{1-\alpha}$ term with \tilde{C}_μ still nonsingular [4]. Such “revised” formulation was later analyzed in the context of Field Theory and the Renormalization Group [41].

The 2000 analysis of two-phase C_V data for CO₂ and propane [5,6] demonstrated that both \tilde{C}_p and \tilde{C}_μ diverge and so implied the existence of the Yang-Yang anomaly. This required scaling theory to be repaired again. The resulting theory, known as “complete scaling” [5,7], is the currently accepted formulation of asymmetric fluid criticality. Under the assumption that all physical fields, p , μ , and T , are “equivalent,” complete scaling predicts a comprehensive set of singularities in the thermodynamic behavior associated with the Yang-Yang anomaly. The most remarkable of them is a new, more dominant $|t|^{2\beta}$ term in the diameter of the coexistence curve whose existence is consistent with experimental data and simulations [11–16].

By introducing a class of lattice-gas-like models called compressible cell gases, Fisher and coworkers [8] provided further support for complete scaling while, at the same time, insights into the microscopic roots of Yang-Yang and related features were revealed. Indeed, such phenomena are due to the *local volumetric effects* inherent to the disordered structure of fluids. More specifically, free volume fluctuations result in YY features, while another source of such phenomena is the coupling between local volumes and energies (as occurs, for instance, for hydrogen bonding in S³D water).

The magnitude of the effects under study are quantified by a single parameter, the YY ratio \mathfrak{R}_μ , which for the models so far considered takes values within $(-\infty, \frac{1}{2})$. This is in reasonable agreement with estimates from experiments and simulations which indicate that \mathfrak{R}_μ typically ranges from negative values of quite small magnitude to values around $\frac{1}{2}$. Finding models—if they exist—yielding $\frac{1}{2} < \mathfrak{R}_\mu < 1$ remains an open task.

The potential applications of compressible cell gases in problems involving anisotropic interactions [42], many-body forces [36], hydrophobic effects [43], fluids in the presence of quenched disorder [44], etc. remain to be assessed. Furthermore, while the concept of complete scaling has been extended to asymmetric liquid-liquid criticality in binary mixtures [45,46] and found to properly describe a wealth of experimental information [45–49], microscopic models for

rationalizing this phenomenology are called for. In another direction, work in order to derive complete scaling from Renormalization Group Theory is currently being reported [50], but more remains to be done on this topic.

ACKNOWLEDGMENTS

This work has been benefited from many significant interactions with Michael E. Fisher, whose encouragement and endless help, including a substantial revision of the manuscript, are greatly appreciated. B. Widom kindly commented on a drafted manuscript. Research by C.A.C. has been supported by the Spanish Ministries of Education, Culture, and Sports (Grant No. PR2006-0449) and of Economy and Competitiveness (Grant No. FIS2011-29614).

APPENDIX A: ISING RESULTS

We make use of the Liu and Fisher [33] results for (1) the dimensionless heat capacity per spin $c \equiv C/\mathcal{N}k_B = (\partial\bar{U}/\partial T)_h/\mathcal{N}k_B$ (with \bar{U} is the internal energy) at $h \equiv H/k_B T = 0$ above (+) and below (−) T_c and (2) the spontaneous magnetization per spin $m_0 \equiv M_0/\mathcal{N}$:

$$c \approx A_I^\pm |\check{K} - 1|^{-\alpha} [1 - a_{\text{eff}}^\pm |\check{K} - 1|^\theta] + b_{\text{eff}}, \quad (\text{A1})$$

$$m_0 \approx B_I |\check{K} - 1|^\beta [1 - a_{\text{eff}} |\check{K} - 1|^\theta], \quad (\text{A2})$$

which are, in fact, the expressions provided by Liu and Fisher but expressed in terms of $\check{K} \equiv K/K_c$, with $K \equiv J/k_B T$. By integrating Eq. (A1) and using $c = -K^2(\partial\bar{u}/\partial K)_{h=0}$, with $\bar{u} \equiv \bar{U}/\mathcal{N}J$, as well as the differential relation

$$d\bar{f} = -\bar{u} dK + m dh, \quad (\text{A3})$$

we get

$$\begin{aligned} \bar{u}^\pm &\approx \bar{u}_c - \frac{b_{\text{eff}}}{K_c} (\check{K} - 1) \pm \frac{A_I^\pm}{K_c(1-\alpha)} |\check{K} - 1|^{1-\alpha} \\ &\quad \times \left[1 - \frac{(1-\alpha)a_{\text{eff}}^\pm}{1+\theta-\alpha} |\check{K} - 1|^\theta \right], \quad (\text{A4}) \\ \bar{f}^\pm &\approx \bar{f}_c - K_c \bar{u}_c (\check{K} - 1) + \frac{b_{\text{eff}}}{2} (\check{K} - 1)^2 \pm \frac{A_I^\pm}{(2-\alpha)(1-\alpha)} \\ &\quad \times |\check{K} - 1|^{2-\alpha} \left[1 - \frac{(2-\alpha)(1-\alpha)a_{\text{eff}}^\pm}{(2+\theta-\alpha)(1+\theta-\alpha)} |\check{K} - 1|^\theta \right], \quad (\text{A5}) \end{aligned}$$

where + and − apply to $T > T_c$ and $T < T_c$, respectively. We have adopted the originally reported [33] numerical values for the critical exponents and critical amplitudes [51].

APPENDIX B: MIXING COEFFICIENTS

We start from

$$\Delta\bar{\beta} = -\bar{\beta}_c t + \bar{\beta}_c t^2 + \dots, \quad (\text{B1})$$

$$\Delta\bar{\rho} = \rho_c \check{\rho} - \bar{\rho}_c t + \bar{\rho}_c t^2 - \rho_c \check{\rho} t + \dots, \quad (\text{B2})$$

$$\Delta\bar{\mu} = \check{\mu} - \left(\frac{\mu_c}{k_B T_c} - \frac{3}{2} \right) t + \left(\frac{\mu_c}{k_B T_c} - \frac{3}{4} \right) t^2 - \check{\mu} t + \dots \quad (\text{B3})$$

Now, by splitting the free energy into its singular and regular parts, i.e., $\bar{f} = \bar{f}^{reg} + \bar{f}^{sing}$, with $\bar{f}^{reg}(K, h) \equiv \bar{f}_c + \bar{f}^{reg}(K, h)$, (3.8) to (3.10) can be put as

$$\begin{aligned} \bar{f}^{sing} = & \bar{f}_\beta^* t + \bar{f}_\mu^* \check{\mu} + \bar{f}_p^* \check{p} + \bar{f}_{\beta\beta}^* t^2 + \bar{f}_{\mu\mu}^* \check{\mu}^2 + \bar{f}_{pp}^* \check{p}^2 \\ & + \bar{f}_{\beta\mu}^* t \check{\mu} + \bar{f}_{\beta p}^* t \check{p} + \bar{f}_{\mu p}^* \check{\mu} \check{p} + \dots - \bar{f}^{reg}, \end{aligned} \quad (\text{B4})$$

$$\begin{aligned} \check{K} - 1 = & \check{K}_\beta^* t + \check{K}_\mu^* \check{\mu} + \check{K}_p^* \check{p} + \check{K}_{\beta\beta}^* t^2 + \check{K}_{\mu\mu}^* \check{\mu}^2 + \check{K}_{pp}^* \check{p}^2 \\ & + \check{K}_{\beta\mu}^* t \check{\mu} + \check{K}_{\beta p}^* t \check{p} + \check{K}_{\mu p}^* \check{\mu} \check{p} + \dots, \end{aligned} \quad (\text{B5})$$

$$\begin{aligned} h = & h_\beta^* t + h_\mu^* \check{\mu} + h_p^* \check{p} + h_{\beta\beta}^* t^2 + h_{\mu\mu}^* \check{\mu}^2 + h_{pp}^* \check{p}^2 \\ & + h_{\beta\mu}^* t \check{\mu} + h_{\beta p}^* t \check{p} + h_{\mu p}^* \check{\mu} \check{p} + \dots. \end{aligned} \quad (\text{B6})$$

Expressions for the coefficients z_β^* , etc., where z can be \bar{f} , \check{K} , or h , are

$$z_\beta^* = -\bar{\beta}_c z_\beta - \left(\frac{\mu_c}{k_B T_c} - \frac{3}{2} \right) z_\mu - \bar{p}_c z_p, \quad (\text{B7})$$

$$z_\mu^* = z_\mu, \quad z_p^* = \rho_c z_p, \quad (\text{B8})$$

$$\begin{aligned} z_{\beta\beta}^* = & \bar{\beta}_c z_\beta + \left(\frac{\mu_c}{k_B T_c} - \frac{3}{4} \right) z_\mu + \bar{p}_c z_p + \frac{1}{2} \bar{\beta}_c^2 z_{\beta\beta} \\ & + \frac{1}{2} \left(\frac{\mu_c}{k_B T_c} - \frac{3}{2} \right)^2 z_{\mu\mu} + \frac{1}{2} \bar{p}_c^2 z_{pp} + \bar{\beta}_c \bar{p}_c z_{\beta p} \\ & + \bar{\beta}_c \left(\frac{\mu_c}{k_B T_c} - \frac{3}{2} \right) z_{\beta\mu} + \bar{p}_c \left(\frac{\mu_c}{k_B T_c} - \frac{3}{2} \right) z_{\mu p}, \end{aligned} \quad (\text{B9})$$

$$z_{\mu\mu}^* = \frac{1}{2} z_{\mu\mu}, \quad z_{pp}^* = \frac{\rho_c^2}{2} z_{pp}, \quad z_{\mu p}^* = \rho_c z_{\mu p}, \quad (\text{B10})$$

$$z_{\beta\mu}^* = -z_\mu - \left(\frac{\mu_c}{k_B T_c} - \frac{3}{2} \right) z_{\mu\mu} - \bar{\beta}_c z_{\beta\mu} - \bar{p}_c z_{\mu p}, \quad (\text{B11})$$

$$z_{\beta p}^* = -\rho_c \left[z_p + \bar{p}_c z_{pp} + \bar{\beta}_c z_{\beta p} + \left(\frac{\mu_c}{k_B T_c} - \frac{3}{2} \right) z_{\mu p} \right]. \quad (\text{B12})$$

Now we recover from (A5) the Ising result for \bar{f}^{reg} at $h = 0$:

$$\bar{f}^{reg} = -K_c \bar{u}_c (\check{K} - 1) + \frac{b_{\text{eff}}}{2} (\check{K} - 1)^2 + \dots, \quad (\text{B13})$$

which, in view of (B5), generates extra terms in (B4) so that

$$\begin{aligned} \bar{f}^{sing} = & (\bar{f}_\beta^* + K_c \bar{u}_c \check{K}_\beta^*) t + (\bar{f}_\mu^* + K_c \bar{u}_c \check{K}_\mu^*) \check{\mu} \\ & + (\bar{f}_p^* + K_c \bar{u}_c \check{K}_p^*) \check{p} + (\bar{f}_{\beta\beta}^* + K_c \bar{u}_c \check{K}_{\beta\beta}^* - \frac{1}{2} b_{\text{eff}} \check{K}_\beta^{*2}) t^2 \\ & + (\bar{f}_{\mu\mu}^* + K_c \bar{u}_c \check{K}_{\mu\mu}^* - \frac{1}{2} b_{\text{eff}} \check{K}_\mu^{*2}) \check{\mu}^2 \\ & + (\bar{f}_{pp}^* + K_c \bar{u}_c \check{K}_{pp}^* - \frac{1}{2} b_{\text{eff}} \check{K}_p^{*2}) \check{p}^2 \\ & + (\bar{f}_{\beta\mu}^* + K_c \bar{u}_c \check{K}_{\beta\mu}^* - b_{\text{eff}} \check{K}_\beta \check{K}_\mu) t \check{\mu} \\ & + (\bar{f}_{\beta p}^* + K_c \bar{u}_c \check{K}_{\beta p}^* - b_{\text{eff}} \check{K}_\beta \check{K}_p) t \check{p} \\ & + (\bar{f}_{\mu p}^* + K_c \bar{u}_c \check{K}_{\mu p}^* - b_{\text{eff}} \check{K}_\mu \check{K}_p) \check{\mu} \check{p} + \dots. \end{aligned} \quad (\text{B14})$$

At this point, we are ready to establish proper connection with Eqs. (2.4)–(2.6). Specifically, by defining

$$\bar{p} \equiv \frac{\bar{f}^{sing}}{\bar{f}_p^* + K_c \bar{u}_c \check{K}_p^*}, \quad \tilde{t} \equiv \frac{\check{K} - 1}{\check{K}_\beta^*}, \quad \tilde{h} \equiv \frac{h}{h_\mu^*}, \quad (\text{B15})$$

one gets

$$k_0 = -\frac{\bar{f}_\beta^* + K_c \bar{u}_c \check{K}_\beta^*}{\bar{f}_p^* + K_c \bar{u}_c \check{K}_p^*}, \quad l_0 = -\frac{\bar{f}_\mu^* + K_c \bar{u}_c \check{K}_\mu^*}{\bar{f}_p^* + K_c \bar{u}_c \check{K}_p^*}, \quad (\text{B16})$$

$$r_0 = -\frac{\bar{f}_{\beta\beta}^* + K_c \bar{u}_c \check{K}_{\beta\beta}^* - b_{\text{eff}} \check{K}_\beta^{*2}/2}{\bar{f}_p^* + K_c \bar{u}_c \check{K}_p^*}, \quad (\text{B17})$$

$$q_0 = -\frac{\bar{f}_{\mu\mu}^* + K_c \bar{u}_c \check{K}_{\mu\mu}^* - b_{\text{eff}} \check{K}_\mu^{*2}/2}{\bar{f}_p^* + K_c \bar{u}_c \check{K}_p^*}, \quad (\text{B18})$$

$$v_0 = -\frac{\bar{f}_{\beta\mu}^* + K_c \bar{u}_c \check{K}_{\beta\mu}^* - b_{\text{eff}} \check{K}_\beta \check{K}_\mu}{\bar{f}_p^* + K_c \bar{u}_c \check{K}_p^*}, \quad (\text{B19})$$

$$m_0 = -\frac{\bar{f}_{pp}^* + K_c \bar{u}_c \check{K}_{pp}^* - b_{\text{eff}} \check{K}_p^{*2}/2}{\bar{f}_p^* + K_c \bar{u}_c \check{K}_p^*}, \quad (\text{B20})$$

$$n_0 = -\frac{\bar{f}_{\beta p}^* + K_c \bar{u}_c \check{K}_{\beta p}^* - b_{\text{eff}} \check{K}_\beta \check{K}_p}{\bar{f}_p^* + K_c \bar{u}_c \check{K}_p^*}, \quad (\text{B21})$$

$$n_3 = -\frac{\bar{f}_{\mu p}^* + K_c \bar{u}_c \check{K}_{\mu p}^* - b_{\text{eff}} \check{K}_\mu \check{K}_p}{\bar{f}_p^* + K_c \bar{u}_c \check{K}_p^*}, \quad (\text{B22})$$

$$l_1 = -\frac{\check{K}_\mu^*}{\check{K}_\beta^*}, \quad j_1 = -\frac{\check{K}_p^*}{\check{K}_\beta^*}, \quad r_1 = -\frac{\check{K}_{\beta\beta}^*}{\check{K}_\beta^*}, \quad (\text{B23})$$

$$q_1 = -\frac{\check{K}_{\mu\mu}^*}{\check{K}_\beta^*}, \quad v_1 = -\frac{\check{K}_{\beta\mu}^*}{\check{K}_\beta^*}, \quad m_1 = -\frac{\check{K}_{pp}^*}{\check{K}_\beta^*}, \quad (\text{B24})$$

$$n_1 = -\frac{\check{K}_{\beta p}^*}{\check{K}_\beta^*}, \quad n_4 = -\frac{\check{K}_{p\mu}^*}{\check{K}_\beta^*}, \quad k_1 = -\frac{h_\beta^*}{h_\mu^*}, \quad (\text{B25})$$

$$j_2 = -\frac{h_p^*}{h_\mu^*}, \quad r_2 = -\frac{h_{\beta\beta}^*}{h_\mu^*}, \quad q_2 = -\frac{h_{\mu\mu}^*}{h_\mu^*}, \quad (\text{B26})$$

$$v_2 = -\frac{h_{\beta\mu}^*}{h_\mu^*}, \quad m_2 = -\frac{h_{pp}^*}{h_\mu^*}, \quad (\text{B27})$$

$$n_2 = -\frac{h_{\beta p}^*}{h_\mu^*}, \quad n_5 = -\frac{h_{p\mu}^*}{h_\mu^*}. \quad (\text{B28})$$

It is important to note that (B16) provides the critical values of the number density and entropy per particle. Specifically, from $l_0 = 1$ and $k_0 = S/\rho_c k_B$, a combination of (B8) and (B16) gives

$$\rho_c = -\frac{\bar{f}_\mu^* + K_c \bar{u}_c \check{K}_\mu^*}{\bar{f}_p^* + K_c \bar{u}_c \check{K}_p^*}, \quad S_c = k_B \frac{\bar{f}_\beta^* + K_c \bar{u}_c \check{K}_\beta^*}{\bar{f}_\mu^* + K_c \bar{u}_c \check{K}_\mu^*}. \quad (\text{B29})$$

APPENDIX C: OTHER RELEVANT AMPLITUDES

Let us now work out the generalized density $\bar{\rho}$ and generalized entropy $\bar{\rho}$, defined from the differential relation

$$d\bar{p} = \bar{\rho} d\tilde{h} + \tilde{s} d\tilde{t}. \quad (\text{C1})$$

From (C1), (A3), and (B15) one gets

$$\bar{\rho} = \left(\frac{\partial \bar{p}}{\partial \tilde{h}} \right)_{\tilde{t}} = \frac{h_\mu^*}{\bar{f}_p^* + K_c \bar{u}_c \check{K}_p^*}, \quad (\text{C2})$$

$$\bar{s} = \left(\frac{\partial \bar{p}}{\partial \bar{t}} \right)_{\bar{h}} = - \frac{\check{K}_\beta^*}{\bar{f}_p^* + K_c \bar{u}_c \check{K}_p^*} \bar{u}. \quad (\text{C3})$$

By using (A2) and (A4), for $h = 0$

$$\bar{\rho} = \pm \frac{h_\mu^*}{\bar{f}_p^* + K_c \bar{u}_c \check{K}_p^*} B_I |\check{K}_\beta^*|^\beta |\bar{t}|^\beta [1 - a_{\text{eff}} |\check{K}_\beta^*|^\theta |\bar{t}|^\theta + \dots], \quad (\text{C4})$$

$$\bar{s} = \pm \left[- \frac{\check{K}_\beta^*}{\bar{f}_p^* + K_c \bar{u}_c \check{K}_p^*} \right] \frac{A_I^\pm}{K_c (1 - \alpha)} |\check{K}_\beta^*|^{1-\alpha} |\bar{t}|^{1-\alpha} \times \left[1 - \frac{a_{\text{eff}}^\pm}{1 + \theta - \alpha} |\check{K}_\beta^*|^\theta |\bar{t}|^\theta + \dots \right], \quad (\text{C5})$$

where + and - in (C4) apply to $h \rightarrow 0^+$ and $h \rightarrow 0^-$ and to $K < K_c$ (or $T > T_c$) and $K > K_c$ (or $T < T_c$) in (C5) By comparing these expressions with those in Ref. [52] we encounter

$$QUW_{-1}^0 = \frac{h_\mu^*}{\bar{f}_p^* + K_c \bar{u}_c \check{K}_p^*} B_I |\check{K}_\beta^*|^\beta, \quad (\text{C6})$$

$$U_{4c} W_{-1}^{(4)} = -a_{\text{eff}} |\check{K}_\beta^*|^\theta, \quad (\text{C7})$$

$$QW_{+0}^0 = - \frac{\check{K}_\beta^*}{\bar{f}_p^* + K_c \bar{u}_c \check{K}_p^*} \frac{A_I^+}{(2 - \alpha)(1 - \alpha)} |\check{K}_\beta^*|^{1-\alpha}, \quad (\text{C8})$$

$$QW_{-0}^0 = - \frac{\check{K}_\beta^*}{\bar{f}_p^* + K_c \bar{u}_c \check{K}_p^*} \frac{A_I^-}{(2 - \alpha)(1 - \alpha)} |\check{K}_\beta^*|^{1-\alpha}, \quad (\text{C9})$$

$$U_{4c} W_{+0}^{(4)} = - \frac{(1 - \alpha) a_{\text{eff}}^+}{(2 + \theta - \alpha)(1 + \theta - \alpha)} |\check{K}_\beta^*|^\theta, \quad (\text{C10})$$

$$U_{4c} W_{-0}^{(4)} = - \frac{(1 - \alpha) a_{\text{eff}}^-}{(2 + \theta - \alpha)(1 + \theta - \alpha)} |\check{K}_\beta^*|^\theta. \quad (\text{C11})$$

APPENDIX D: RESULTS FOR CCG₀ AND RELATED MODELS

Here we provide specific results for the basic CCG₀ model, the CCG₀⁺, and the “simplest” decorated CCG₀ described in Secs. III and IV. Concretely, we show the analytic expressions of the functions $g_i(\bar{\beta}_c, \bar{\mu}_c, \bar{p}_c)$ ($i = 1, 2, 3$) defined in (3.11) as well as the derivatives \bar{f}_β , etc. defined in Appendix B. While not explicitly stated here but noted in the main body of the text, S_{ij} are evaluated at $\bar{p} = \bar{p}_c$ and S_{ijk}^+ at $\bar{p} = \bar{p}_c$ and $\bar{\beta} = \bar{\beta}_c$.

For the CCG₀, presented in Sec. III A, one has

$$g_1(\bar{\beta}_c, \bar{\mu}_c, \bar{p}_c) = - \frac{c}{8} \bar{\beta}_c \varepsilon_0 - \frac{1}{2} \bar{\mu}_c - \frac{1}{2} \ln \left(\frac{S_{01} S_{00}}{v_0} \right), \quad (\text{D1})$$

$$g_2(\bar{\beta}_c) = \frac{1}{4K_c} \bar{\beta}_c \varepsilon_0, \quad (\text{D2})$$

$$g_3(\bar{\beta}_c, \bar{\mu}_c, \bar{p}_c) = \frac{1}{2} \bar{\mu}_c + \frac{c}{4} \bar{\beta}_c \varepsilon_0 + \frac{1}{2} \ln \left(\frac{S_{01}}{v_0 S_{00}} \right), \quad (\text{D3})$$

$$\bar{f}_\beta = - \frac{c\varepsilon_0}{8}, \quad \bar{f}_\mu = - \frac{1}{2}, \quad \bar{f}_p = \frac{1}{2} \left(\frac{S_{10}}{S_{00}} + \frac{S_{11}}{S_{01}} \right), \quad (\text{D4})$$

$$\check{K}_\beta = \frac{\varepsilon_0}{4K_c}, \quad \check{K}_\mu = 0, \quad \check{K}_p = 0, \quad (\text{D5})$$

$$h_\beta = \frac{c\varepsilon_0}{4}, \quad h_\mu = \frac{1}{2}, \quad h_p = \frac{1}{2} \left(\frac{S_{10}}{S_{00}} - \frac{S_{11}}{S_{01}} \right), \quad (\text{D6})$$

$$\bar{f}_{pp} = \frac{1}{2} \left[\left(\frac{S_{11}}{S_{01}} \right)^2 + \left(\frac{S_{10}}{S_{00}} \right)^2 - \left(\frac{S_{21}}{S_{01}} + \frac{S_{20}}{S_{00}} \right) \right], \quad (\text{D7})$$

$$h_{pp} = \frac{1}{2} \left[\left(\frac{S_{10}}{S_{00}} \right)^2 - \left(\frac{S_{11}}{S_{01}} \right)^2 + \left(\frac{S_{21}}{S_{01}} - \frac{S_{20}}{S_{00}} \right) \right], \quad (\text{D8})$$

$$\bar{f}_{\beta\beta} = \bar{f}_{\mu\mu} = \bar{f}_{\beta\mu} = \bar{f}_{\beta p} = \bar{f}_{\mu p} = 0, \quad (\text{D9})$$

$$\check{K}_{\beta\beta} = \check{K}_{\mu\mu} = \check{K}_{pp} = \check{K}_{\beta\mu} = \check{K}_{\beta p} = \check{K}_{\mu p} = 0, \quad (\text{D10})$$

$$h_{\beta\beta} = h_{\mu\mu} = h_{\beta\mu} = h_{\beta p} = h_{\mu p} = 0. \quad (\text{D11})$$

Here are the results for the CCG₀⁺, described in Sec. III D:

$$g_1(\bar{\beta}_c, \bar{\mu}_c, \bar{p}_c) = - \frac{c}{8} \bar{\beta}_c \varepsilon_0 - \frac{1}{2} \bar{\mu}_c - \frac{1}{2} \ln \left(\frac{S_{010}^+ S_{00}}{v_0} \right), \quad (\text{D12})$$

$$g_2(\bar{\beta}_c) = \frac{1}{4K_c} \bar{\beta}_c \varepsilon_0, \quad (\text{D13})$$

$$g_3(\bar{\beta}_c, \bar{\mu}_c, \bar{p}_c) = \frac{1}{2} \bar{\mu}_c + \frac{c}{4} \bar{\beta}_c \varepsilon_0 + \frac{1}{2} \ln \left(\frac{S_{010}^+}{v_0 S_{00}} \right), \quad (\text{D14})$$

$$\bar{f}_\beta = - \frac{c\varepsilon_0}{8} + \frac{1}{2} \frac{S_{011}^+}{S_{010}^+}, \quad \bar{f}_\mu = - \frac{1}{2}, \quad \bar{f}_p = \frac{1}{2} \left(\frac{S_{10}}{S_{00}} + \frac{S_{110}^+}{S_{010}^+} \right), \quad (\text{D15})$$

$$\check{K}_\beta = \frac{\varepsilon_0}{4K_c}, \quad \check{K}_\mu = 0, \quad \check{K}_p = 0, \quad (\text{D16})$$

$$h_\beta = \frac{c\varepsilon_0}{4} - \frac{1}{2} \frac{S_{011}^+}{S_{010}^+}, \quad h_\mu = \frac{1}{2}, \quad h_p = \frac{1}{2} \left(\frac{S_{10}}{S_{00}} - \frac{S_{110}^+}{S_{010}^+} \right), \quad (\text{D17})$$

$$\bar{f}_{pp} = \frac{1}{2} \left[\left(\frac{S_{10}}{S_{00}} \right)^2 + \left(\frac{S_{110}^+}{S_{010}^+} \right)^2 - \left(\frac{S_{210}^+}{S_{010}^+} + \frac{S_{20}}{S_{00}} \right) \right], \quad (\text{D18})$$

$$h_{pp} = \frac{1}{2} \left[\left(\frac{S_{10}}{S_{00}} \right)^2 - \left(\frac{S_{110}^+}{S_{010}^+} \right)^2 + \left(\frac{S_{210}^+}{S_{010}^+} - \frac{S_{20}}{S_{00}} \right) \right], \quad (\text{D19})$$

$$\bar{f}_{\beta\beta} = \frac{1}{2} \left[\left(\frac{S_{011}^+}{S_{010}^+} \right)^2 - \frac{S_{012}^+}{S_{010}^+} \right], \quad (\text{D20})$$

$$\bar{f}_{\beta p} = \frac{1}{2} \left[\frac{S_{110}^+ S_{011}^+}{(S_{010}^+)^2} - \frac{S_{111}^+}{S_{010}^+} \right], \quad (\text{D21})$$

$$\bar{f}_{\mu\mu} = \bar{f}_{\beta\mu} = \bar{f}_{\mu p} = 0, \quad (\text{D22})$$

$$\check{K}_{\beta\beta} = \check{K}_{\mu\mu} = \check{K}_{pp} = \check{K}_{\beta\mu} = \check{K}_{\beta p} = \check{K}_{\mu p} = 0, \quad (\text{D23})$$

$$h_{\beta\beta} = -\bar{f}_{\beta\beta}, \quad h_{\beta p} = -\bar{f}_{\beta p}, \quad h_{\mu\mu} = h_{\beta\mu} = h_{\mu p} = 0. \quad (\text{D24})$$

Finally, for the ‘‘simplest’’ decorated CCG₀ presented in Sec. IV B:

$$g_1(\bar{\beta}_c, \bar{\mu}_c, \bar{p}_c) = -\frac{c}{8}\bar{\beta}_c\varepsilon_0 - \frac{1}{2}\bar{\mu}_c - \frac{1}{2}\ln\left(\frac{S_{01}S_{00}}{v_0}\right) - \frac{c}{8}\ln\left[\left(S_{00} + \frac{1}{v_0}S_{01}e^{2\bar{\beta}_c\varepsilon_0 + \bar{\mu}_c}\right)\left(S_{00} + \frac{1}{v_0}S_{01}e^{\bar{\mu}_c}\right)\left(S_{00} + \frac{1}{v_0}S_{01}e^{\bar{\beta}_c\varepsilon_0 + \bar{\mu}_c}\right)^2\right], \quad (\text{D25})$$

$$g_2(\bar{\beta}_c) = \frac{1}{4K_c}\bar{\beta}_c\varepsilon_0 + \frac{1}{4K_c}\ln\left[\frac{\left(S_{00} + \frac{1}{v_0}S_{01}e^{2\bar{\beta}_c\varepsilon_0 + \bar{\mu}_c}\right)\left(S_{00} + \frac{1}{v_0}S_{01}e^{\bar{\mu}_c}\right)}{\left(S_{00} + \frac{1}{v_0}S_{01}e^{\bar{\beta}_c\varepsilon_0 + \bar{\mu}_c}\right)^2}\right], \quad (\text{D26})$$

$$g_3(\bar{\beta}_c, \bar{\mu}_c, \bar{p}_c) = \frac{1}{2}\bar{\mu}_c + \frac{c}{4}\bar{\beta}_c\varepsilon_0 + \frac{1}{2}\ln\left(\frac{S_{01}}{v_0S_{00}}\right) + \frac{c}{4}\ln\left(\frac{S_{00} + \frac{1}{v_0}S_{01}e^{2\bar{\beta}_c\varepsilon_0 + \bar{\mu}_c}}{S_{00} + \frac{1}{v_0}S_{01}e^{\bar{\mu}_c}}\right), \quad (\text{D27})$$

$$\bar{f}_\beta = -\frac{c\varepsilon_0}{8} - \frac{c\varepsilon_0S_{01}}{4v_0}\left(\frac{e^{2\bar{\beta}_c + \bar{\mu}}}{S_{00} + \frac{1}{v_0}S_{01}e^{2\bar{\beta}_c + \bar{\mu}}} + \frac{e^{\bar{\beta}_c + \bar{\mu}}}{S_{00} + \frac{1}{v_0}S_{01}e^{\bar{\beta}_c + \bar{\mu}}}\right), \quad (\text{D28})$$

$$\bar{f}_\mu = -\frac{1}{2} - \frac{c}{8}\left(\frac{\frac{1}{v_0}S_{01}e^{2\bar{\beta}_c\varepsilon_0 + \bar{\mu}}}{S_{00} + \frac{1}{v_0}S_{01}e^{2\bar{\beta}_c\varepsilon_0 + \bar{\mu}}} + \frac{\frac{1}{v_0}S_{01}e^{\bar{\mu}}}{S_{00} + \frac{1}{v_0}S_{01}e^{\bar{\mu}}} + 2\frac{\frac{1}{v_0}S_{01}e^{\bar{\beta}_c\varepsilon_0 + \bar{\mu}}}{S_{00} + \frac{1}{v_0}S_{01}e^{\bar{\beta}_c\varepsilon_0 + \bar{\mu}}}\right), \quad (\text{D29})$$

$$\bar{f}_p = \frac{1}{2}\left(\frac{S_{11}}{S_{01}} + \frac{S_{10}}{S_{00}}\right) + \frac{c}{8}\left(\frac{S_{10} + \frac{1}{v_0}S_{11}e^{2\bar{\beta}_c\varepsilon_0 + \bar{\mu}}}{S_{00} + \frac{1}{v_0}S_{01}e^{2\bar{\beta}_c\varepsilon_0 + \bar{\mu}}} + \frac{S_{10} + \frac{1}{v_0}S_{11}e^{\bar{\mu}}}{S_{00} + \frac{1}{v_0}S_{01}e^{\bar{\mu}}} + 2\frac{S_{10} + \frac{1}{v_0}S_{11}e^{\bar{\beta}_c\varepsilon_0 + \bar{\mu}}}{S_{00} + \frac{1}{v_0}S_{01}e^{\bar{\beta}_c\varepsilon_0 + \bar{\mu}}}\right), \quad (\text{D30})$$

$$\check{K}_\beta = \frac{\varepsilon_0}{4K_c} + \frac{\varepsilon_0S_{01}}{2K_cv_0}\left(\frac{e^{2\bar{\beta}_c + \bar{\mu}}}{S_{00} + \frac{1}{v_0}S_{01}e^{2\bar{\beta}_c + \bar{\mu}}} - \frac{e^{\bar{\beta}_c + \bar{\mu}}}{S_{00} + \frac{1}{v_0}S_{01}e^{\bar{\beta}_c + \bar{\mu}}}\right), \quad (\text{D31})$$

$$\check{K}_\mu = \frac{1}{4}\left[\frac{\frac{1}{v_0}S_{01}e^{2\bar{\beta}_c\varepsilon_0 + \bar{\mu}}}{S_{00} + \frac{1}{v_0}S_{01}e^{2\bar{\beta}_c\varepsilon_0 + \bar{\mu}}} + \frac{\frac{1}{v_0}S_{01}e^{\bar{\mu}}}{S_{00} + \frac{1}{v_0}S_{01}e^{\bar{\mu}}} - 2\frac{\frac{1}{v_0}S_{01}e^{\bar{\beta}_c\varepsilon_0 + \bar{\mu}}}{S_{00} + \frac{1}{v_0}S_{01}e^{\bar{\beta}_c\varepsilon_0 + \bar{\mu}}}\right], \quad (\text{D32})$$

$$\check{K}_p = -\frac{1}{4}\left[\frac{S_{10} + \frac{1}{v_0}S_{11}e^{2\bar{\beta}_c\varepsilon_0 + \bar{\mu}}}{S_{00} + \frac{1}{v_0}S_{01}e^{2\bar{\beta}_c\varepsilon_0 + \bar{\mu}}} + \frac{S_{10} + \frac{1}{v_0}S_{11}e^{\bar{\mu}}}{S_{00} + \frac{1}{v_0}S_{01}e^{\bar{\mu}}} - 2\frac{S_{10} + \frac{1}{v_0}S_{11}e^{\bar{\beta}_c\varepsilon_0 + \bar{\mu}}}{S_{00} + \frac{1}{v_0}S_{01}e^{\bar{\beta}_c\varepsilon_0 + \bar{\mu}}}\right], \quad (\text{D33})$$

$$h_\beta = \frac{c\varepsilon_0}{4} + \frac{c\varepsilon_0S_{01}}{4v_0}\left(\frac{2e^{2\bar{\beta}_c + \bar{\mu}}}{S_{00} + \frac{1}{v_0}S_{01}e^{2\bar{\beta}_c + \bar{\mu}}} - \frac{e^{\bar{\beta}_c + \bar{\mu}}}{S_{00} + \frac{1}{v_0}S_{01}e^{\bar{\beta}_c + \bar{\mu}}}\right), \quad (\text{D34})$$

$$h_\mu = \frac{1}{2} + \frac{c}{4}\left(\frac{\frac{1}{v_0}S_{01}e^{2\bar{\beta}_c\varepsilon_0 + \bar{\mu}}}{S_{00} + \frac{1}{v_0}S_{01}e^{2\bar{\beta}_c\varepsilon_0 + \bar{\mu}}} - \frac{\frac{1}{v_0}S_{01}e^{\bar{\mu}}}{S_{00} + \frac{1}{v_0}S_{01}e^{\bar{\mu}}}\right), \quad (\text{D35})$$

$$h_p = \frac{1}{2}\left(\frac{S_{10}}{S_{00}} - \frac{S_{11}}{S_{01}}\right) - \frac{c}{4}\left(\frac{S_{10} + \frac{1}{v_0}S_{11}e^{2\bar{\beta}_c\varepsilon_0 + \bar{\mu}}}{S_{00} + \frac{1}{v_0}S_{01}e^{2\bar{\beta}_c\varepsilon_0 + \bar{\mu}}} - \frac{S_{10} + \frac{1}{v_0}S_{11}e^{\bar{\mu}}}{S_{00} + \frac{1}{v_0}S_{01}e^{\bar{\mu}}}\right). \quad (\text{D36})$$

APPENDIX E: RESULTS FOR THE SASTRY-DEBENEDETTI-SCIORTINO-STANLEY MODEL

Information for the S³D model, described in Sec. IV C, is the following:

$$g_1 = -\frac{c}{2}\ln q - \frac{c}{8}\bar{\beta}_c\varepsilon_0 - \frac{1}{2}\bar{\mu}_c + \bar{p}_c - \frac{c}{8}\ln\left(1 + \frac{e^{\bar{\beta}_c\delta\varepsilon - \bar{p}_cv_+} - 1}{q}\right), \quad (\text{E1})$$

$$g_2 = \frac{1}{4K_c}\bar{\beta}_c\varepsilon_0 + \frac{1}{4K_c}\ln\left(1 + \frac{e^{\bar{\beta}_c\delta\varepsilon - \bar{p}_cv_+} - 1}{q}\right), \quad (\text{E2})$$

$$g_3 = \frac{c}{2}\ln q + \frac{c}{4}\bar{\beta}_c\varepsilon_0 + \frac{1}{2}\bar{\mu}_c + \frac{c}{4}\ln\left(1 + \frac{e^{\bar{\beta}_c\delta\varepsilon - \bar{p}_cv_+} - 1}{q}\right), \quad (\text{E3})$$

$$\bar{f}_\beta = -\frac{c}{8}\left(\varepsilon_0 + \frac{\delta\varepsilon e^{\bar{\beta}_c\delta\varepsilon - \bar{p}_cv_+}}{q - 1 + e^{\bar{\beta}_c\delta\varepsilon - \bar{p}_cv_+}}\right), \quad \bar{f}_\mu = -\frac{1}{2}, \quad (\text{E4})$$

$$\bar{f}_p = 1 + \frac{cv_+ e^{\bar{\beta}_c\delta\varepsilon - \bar{p}_cv_+}}{8(q - 1 + e^{\bar{\beta}_c\delta\varepsilon - \bar{p}_cv_+})}, \quad (\text{E5})$$

$$\check{K}_\beta = \frac{1}{4K_c}\left(\varepsilon_0 + \frac{\delta\varepsilon e^{\bar{\beta}_c\delta\varepsilon - \bar{p}_cv_+}}{q - 1 + e^{\bar{\beta}_c\delta\varepsilon - \bar{p}_cv_+}}\right), \quad \check{K}_\mu = 0, \quad (\text{E6})$$

$$\check{K}_p = -\frac{v_+ e^{\bar{\beta}_c\delta\varepsilon - \bar{p}_cv_+}}{4K_c(q - 1 + e^{\bar{\beta}_c\delta\varepsilon - \bar{p}_cv_+})}, \quad (\text{E7})$$

$$h_\beta = \frac{c}{4}\left(\varepsilon_0 + \frac{\delta\varepsilon e^{\bar{\beta}_c\delta\varepsilon - \bar{p}_cv_+}}{q - 1 + e^{\bar{\beta}_c\delta\varepsilon - \bar{p}_cv_+}}\right), \quad h_\mu = \frac{1}{2}, \quad (\text{E8})$$

$$h_p = -\frac{c v_+ e^{\bar{\beta}_c \delta \varepsilon - \bar{p}_c v_+}}{4(q-1 + e^{\bar{\beta}_c \delta \varepsilon - \bar{p}_c v_+})}, \quad (\text{E9})$$

$$\bar{f}_{\beta\beta} = -\frac{c \delta \varepsilon^2 (q-1) e^{\bar{\beta}_c \delta \varepsilon - \bar{p}_c v_+}}{8(q-1 + e^{\bar{\beta}_c \delta \varepsilon - \bar{p}_c v_+})^2}, \quad (\text{E10})$$

$$\bar{f}_{pp} = \bar{f}_{\beta\beta} \left(\frac{v_+}{\delta \varepsilon} \right)^2, \quad f_{\beta p} = \bar{f}_{\beta\beta} \frac{v_+}{\delta \varepsilon}, \quad (\text{E11})$$

$$\check{K}_{\beta\beta} = \frac{\delta \varepsilon^2 (q-1) e^{\bar{\beta}_c \delta \varepsilon - \bar{p}_c v_+}}{4K_c (q-1 + e^{\bar{\beta}_c \delta \varepsilon - \bar{p}_c v_+})^2}, \quad (\text{E12})$$

$$\check{K}_{pp} = \check{K}_{\beta\beta} \left(\frac{v_+}{\delta \varepsilon} \right)^2, \quad \check{K}_{\beta p} = \check{K}_{\beta\beta} \frac{v_+}{\delta \varepsilon}, \quad (\text{E13})$$

$$h_{\beta\beta} = \frac{c \delta \varepsilon^2 (q-1) e^{\bar{\beta}_c \delta \varepsilon - \bar{p}_c v_+}}{4(q-1 + e^{\bar{\beta}_c \delta \varepsilon - \bar{p}_c v_+})^2}, \quad (\text{E14})$$

$$h_{pp} = h_{\beta\beta} \left(\frac{v_+}{\delta \varepsilon} \right)^2, \quad h_{\beta p} = h_{\beta\beta} \frac{v_+}{\delta \varepsilon}, \quad (\text{E15})$$

$$\bar{f}_{\beta\mu} = \bar{f}_{\mu\mu} = \bar{f}_{\mu p} = \check{K}_{\beta\mu} = \check{K}_{\mu\mu} = \check{K}_{\mu p} 0. \quad (\text{E16})$$

$$h_{\beta\mu} = h_{\mu\mu} = h_{\mu p} = 0. \quad (\text{E17})$$

- [1] See for review M. E. Fisher in *Critical Phenomena*, edited by F. J. W. Hahne, Lecture Notes in Physics Vol. 186 (Springer-Verlag, New York, 1982), pp. 1–139.
- [2] C. N. Yang and C. P. Yang, *Phys. Rev. Lett.* **13**, 303 (1964).
- [3] B. Widom, *J. Chem. Phys.* **43**, 3898 (1965).
- [4] See, e.g., J. J. Rehr and N. D. Mermin, *Phys. Rev. A* **8**, 472 (1973).
- [5] M. E. Fisher and G. Orkoulas, *Phys. Rev. Lett.* **85**, 696 (2000).
- [6] G. Orkoulas, M. E. Fisher, and C. Üstün, *J. Chem. Phys.* **113**, 7530 (2000).
- [7] Y. C. Kim, M. E. Fisher, and G. Orkoulas, *Phys. Rev. E* **67**, 061506 (2003).
- [8] C. A. Cerdeiriña, G. Orkoulas, and M. E. Fisher, *Phys. Rev. Lett.* **116**, 040601 (2016).
- [9] I. M. Abdulagatov, N. G. Polikhronidi, and R. G. Batyrova, *Fluid Phase Equilib.* **415**, 144 (2016).
- [10] As noted in Sec. II A, complete scaling also contemplates the existence of a linear term in the diameter.
- [11] Y. C. Kim and M. E. Fisher, *Chem. Phys. Lett.* **414**, 185 (2005).
- [12] M. A. Anisimov and J. Wang, *Phys. Rev. Lett.* **97**, 025703 (2006).
- [13] J. Wang and M. A. Anisimov, *Phys. Rev. E* **75**, 051107 (2007).
- [14] Y. C. Kim, *Phys. Rev. E* **71**, 051501 (2005).
- [15] L. Li, K. Tang, L. Wu, W. Zhao, and J. Cai, *J. Chem. Phys.* **136**, 214508 (2012).
- [16] L. Li, F. Sun, Z. Chen, L. Wang, and J. Cai, *J. Chem. Phys.* **141**, 054905 (2014).
- [17] T. D. Lee and C. N. Yang, *Phys. Rev.* **87**, 410 (1952).
- [18] Ref. [17] shows that the SLG and the Ising model are mathematically equivalent. In this regard, while the SLG largely improves van der Waals mean-field theory because, via the results for the Ising model, it yields the right, nonclassical values for critical exponents, it may be regarded as clearly inappropriate in connection with asymmetry since its coexistence curve is fully symmetric. Note that the original vdW approach, characterized by a rectilinear diameter with a nonvanishing slope, supports an asymmetric coexistence curve.
- [19] B. Widom and J. S. Rowlinson, *J. Chem. Phys.* **52**, 1670 (1970).
- [20] N. D. Mermin, *Phys. Rev. Lett.* **26**, 957 (1971).
- [21] See E. A. Guggenheim, *Thermodynamics*, 2nd ed. (North-Holland, Amsterdam, 1950), Sec. 2.08.
- [22] R. A. Sack, *Mol. Phys.* **2**, 8 (1959), and references therein.
- [23] M. E. Fisher, *Phys. Rev.* **113**, 969 (1959).
- [24] C. Domb, *Adv. Phys.* **9**, 149 (1960).
- [25] S. Sastry, P. G. Debenedetti, F. Sciortino, and H. E. Stanley, *Phys. Rev. E* **53**, 6144 (1996).
- [26] As is common usage in the thermodynamics of critical phenomena, we employ here the term “fields” to design those thermodynamic variables which, in contrast to “densities,” take the same values for the coexisting phases [1].
- [27] M. E. Fisher and Y. C. Kim, *J. Chem. Phys.* **117**, 779 (2002).
- [28] One can find in Ref. [7] the expressions that complete scaling provides for the heat capacity and its components in the one-phase region ($T > T_c$).
- [29] An entirely equivalent derivation can be carried out by starting from the isothermal-isobaric (N, p, T) ensemble and, then, performing a summation over N to get $\Theta(\mu, p, T)$.
- [30] Note that for a CCG₀ of noninteracting particles $\Theta_N = \Theta_1^N$, with Θ_1 the single-cell partition function. By introducing this result into (2.26) one finds $\Theta = 1/(1 - \Theta_1)$, implying that $\Theta_1 = 1$ because the partition function diverges. The prefactor n^{-1} in (3.4) is, therefore, needed to get $\Theta_1 = 1$ in the ideal-gas limit ($p \rightarrow 0, \mu \rightarrow -\infty$).
- [31] Note that $S_{01}/S_{00} = v_0$ for the standard lattice gas, so that this model does not display pressure mixing into \tilde{h} .
- [32] Pressure mixing was originally noted in *one-dimensional cluster interaction models* [M. E. Fisher and B. U. Felderhof, *Ann. Phys. (N. Y.)* **58**, 217 (1970), Secs. 8, 9] which were, however, viewed as “peculiar.”
- [33] A. J. Liu and M. E. Fisher, *Physica A* **156**, 35 (1989).
- [34] In order to convert $\bar{\mu}_c$, defined just below (3.1), to $\mu_c/k_B T_c$, values for v_0, ε_0 , and $\Lambda_T(T_c)$ need to be specified. Properties of a reference fluid were taken for that purpose. A typical value for v_0 was obtained from the volume per particle of argon at the triple point, a high-density thermodynamic state in which, to a reasonable approximation, particles are close enough so that almost all cells of a hypothetical lattice gas would be occupied; the value of this volume per particle has been taken from the NIST Chemistry WebBook Database (<http://webbook.nist.gov/chemistry/>). As for ε_0 , the minimum of the Lennard-Jones pair potential of that fluid was adopted; this has been taken from page 6 in J.-P. Hansen and I. R. McDonald, *Theory of Simple Liquids*, 3rd ed. (Elsevier, Amsterdam, 2006). Then $\Lambda_T(T_c)$, which can be expressed as $\Lambda_T(T_c) = l^* \bar{\beta}_c^{1/2}$, with $l^* = h/(2\pi m \varepsilon_0)^{1/2}$, is determined by simply using the atomic mass of argon. Adopted values are $\varepsilon_0 = 1000 \text{ J mol}^{-1}$, $v_0 = 5 \times 10^{-29} \text{ m}^3$, and $l^* = 2.5 \times 10^{-11} \text{ m}$.

- [35] J. C. Wheeler, *Annu. Rev. Phys. Chem.* **28**, 411 (1977).
- [36] M. W. Pestak, R. E. Goldstein, M. H. W. Chan, J. R. de Bruyn, D. A. Balzarini, and N. W. Ashcroft, *Phys. Rev. B* **36**, 599 (1987).
- [37] In general [23,24] a function, say, Π , relating the summations for a vertex-decorating cell assembly (like that depicted in Fig. 5) with those for two nearest-neighbor cells of the undecorated model is needed. If we denote the GGC partition functions of the decorated model and the undecorated CCG₀ as $\Theta_{\mathcal{N}}^{\text{d-CCG}}$ and $\Theta_{\mathcal{N}}^{\text{CCG}_0}$, one has $\Theta_{\mathcal{N}}^{\text{d-CCG}} = \Pi^{c_{\mathcal{N}}/2} \Theta_{\mathcal{N}}^{\text{CCG}_0}$. But taking into account that both partition functions equate to unity provided \mathcal{N} is large enough, this implies that $\Pi = 1$. This is a specific feature of the decoration transformation in the GGC ensemble.
- [38] C. A. Angell, *Ann. Rev. Phys. Chem.* **34**, 593 (1983); O. Mishima and H. E. Stanley, *Nature (London)* **396**, 329 (1998); P. G. Debenedetti, *J. Phys.: Condens. Matter* **15**, R1669 (2003).
- [39] M. I. Bagatskii, A. V. Voronel, and V. G. Gusak, *Zh. Eksp. Teor. Fiz.* **43**, 728 (1962) [*Sov. Phys. JETP* **16**, 517 (1963)].
- [40] J. Weiner, K. H. Langley, and N. C. Ford, *Phys. Rev. Lett.* **32**, 879 (1974).
- [41] J. F. Nicoll, *Phys. Rev. A* **24**, 2203 (1981); M. Ley-Koo and M. S. Green, *ibid.* **23**, 2650 (1981).
- [42] M. E. Fisher, *Proc. R. Soc. A* **254**, 66 (1960); **256**, 502 (1960).
- [43] B. Widom, P. Bhimalapuram, and K. Koga, *Phys. Chem. Chem. Phys.* **5**, 3085 (2003).
- [44] G. Pellicane, R. L. C. Vink, B. Russo, and P. V. Giaquinta, *Phys. Rev. E* **88**, 042131 (2013).
- [45] C. A. Cerdeiriña, M. A. Anisimov, and J. V. Sengers, *Chem. Phys. Lett.* **424**, 414 (2006); J. Wang, C. A. Cerdeiriña, M. A. Anisimov, and J. V. Sengers, *Phys. Rev. E* **77**, 031127 (2008); G. Pérez-Sánchez, P. Losada-Pérez, C. A. Cerdeiriña, J. V. Sengers, and M. A. Anisimov, *J. Chem. Phys.* **132**, 154502 (2010).
- [46] P. Losada-Pérez, G. Pérez-Sánchez, C. A. Cerdeiriña, and J. Thoen, *Phys. Rev. E* **81**, 041121 (2010); C. E. Bertrand, J. V. Sengers, and M. A. Anisimov, *J. Phys. Chem. B* **115**, 14000 (2011).
- [47] P. Losada-Pérez, C. S. P. Tripathy, J. Leys, C. A. Cerdeiriña, C. Glorieux, and J. Thoen, *Chem. Phys. Lett.* **523**, 69 (2012).
- [48] P. Losada-Pérez, C. Glorieux, and J. Thoen, *J. Chem. Phys.* **136**, 144502 (2012).
- [49] T. Yin, S. Liu, J. Xie, and W. Shen, *J. Chem. Phys.* **138**, 024504 (2013).
- [50] See, e.g., L. Wang, W. Zhao, L. Wu, L. Li, and J. Cai, *J. Chem. Phys.* **139**, 124103 (2013); A. S. V. Ramana, *Physica A* **442**, 137 (2016).
- [51] The value of b_{eff} was fixed to the arithmetic mean of b_{eff}^+ and b_{eff}^- in Ref. [32].
- [52] Section (3.2.4) in Y. C. Kim, Ph.D. thesis, University of Maryland, 2002.